Climatic variability
Cloud-top temperature/height
The autumn of 1987
Modelling precipitation
W.H. Hogg — an appreciation
Groves Prizes and Awards

THE METEOROLOGICAL MAGAZINE

HER MAJESTY'S
STATIONERY
OFFICE

July 1988

Met.O.982 No. 1392 Vol. 117

THE METEOROLOGICAL MAGAZINE

No. 1392, July 1988, Vol. 117

551.583

The nature of climatic variability

D.E. Parker and C.K. Folland

Meteorological Office, Bracknell

Summary

Climatic variability results not only from the complex dynamics of the atmosphere but also from feedbacks involving the atmosphere, the oceans, the biosphere, and ice and snow. External influences such as solar changes, volcanic eruptions, and man-made pollution may also influence climate. Observed variations range in time-scale from daily weather fluctuations to pronounced interdecadal changes of temperature, rainfall and atmospheric circulation. The longer-term changes may involve changes in variability as well as in average conditions. Except for the very shortest time-scales, local and regional variations of weather and climate cannot be understood without considering the whole globe.

Examples of observed climatic variations are used to amplify the above remarks. The possibility of climatic prediction is discussed. Improved understanding of the earth's complex climatic system is a prerequisite for useful climatic prediction, and the need for much further observational and modelling research is clear.

1. Introduction

The subject of climatic variability is a difficult one to outline. There is no precise boundary between short-term variability consisting of spells, months or seasons of differing character, which can be regarded as a natural part of a fixed climate, and long-term variability, which involves changes in the frequencies and mean values of climatic quantities (e.g. values of temperature, rainfall, patterns of atmospheric pressure) over periods of several decades or longer. The complexity of the subject is increased by the fact that long-term variability can show itself not only as a change in the average value of a climatic variable (e.g. a warming or a drying trend) but also as a modulation of the short-term variability that is inherent in the climate (e.g. a changed likelihood of extremes). This paper illustrates several different types of climatic variability in an attempt to clarify some of these issues.

Climatic variability is predominantly irregular. Apart from the annual and diurnal cycles, there are few proven regular periodicities in the atmosphere, and most of these are in the stratosphere or above. The characteristic irregularity of climatic variability results from the large number of physical processes that contribute to the earth's climatic system which includes the oceans, biosphere and cryosphere (snow and ice) as well as the atmosphere. Climate may also be affected by additional influences such as solar changes, volcanic eruptions and man-made pollution. A consequence of this complexity is that it is at present especially difficult or impossible to predict details of future local or regional climate. Statistical

extrapolation of trends or recurrent tendencies in the climate is scientifically unsound to the extent that it fails to take account of the competing physical processes involved, though occasional limited successes have been achieved. The use of numerical models encapsulating the physical processes occurring world-wide should provide the firmest foundation for progress. Such models are extremely complex and their present state of development, while allowing generalized predictions on a global scale (e.g. of globally averaged surface warming resulting from increased atmospheric carbon dioxide), is still inadequate for confident prediction of future changes in local and regional climate. This limitation is underlined by the inability of the models to reproduce precisely the present climate — including its inherent short-term variability, though some progress is now being made (see section 4).

2. Short-term variability

Weather fluctuations, and short and long spells of differing or unusual character, are illustrated by the sequence of daily 'Central England Temperature' for 1986 in Fig. 1. Central England Temperature (see, for example, Manley 1974, Jones 1987) is computed by averaging daily maximum and minimum temperatures for several stations in an area stretching from the south Midlands to south Lancashire. Fig. 1 includes the climatological averages for 1951–80, so that daily deviations from normal can be seen clearly. For individual stations in England, the daily deviations are similar to those in the Central England Temperature sequence, but are not identical; individual locations tend to show slightly more variability, which is smoothed out by the averaging, and there are variations across country according to weather type.

Marked irregular fluctuations ranging from a few days to over a month's duration are evident in Fig. 1. The existence of a number of coherent atmospheric patterns, whose scale is of the order of several thousand kilometres and which repeat in approximately the same form with lifetimes of the order of

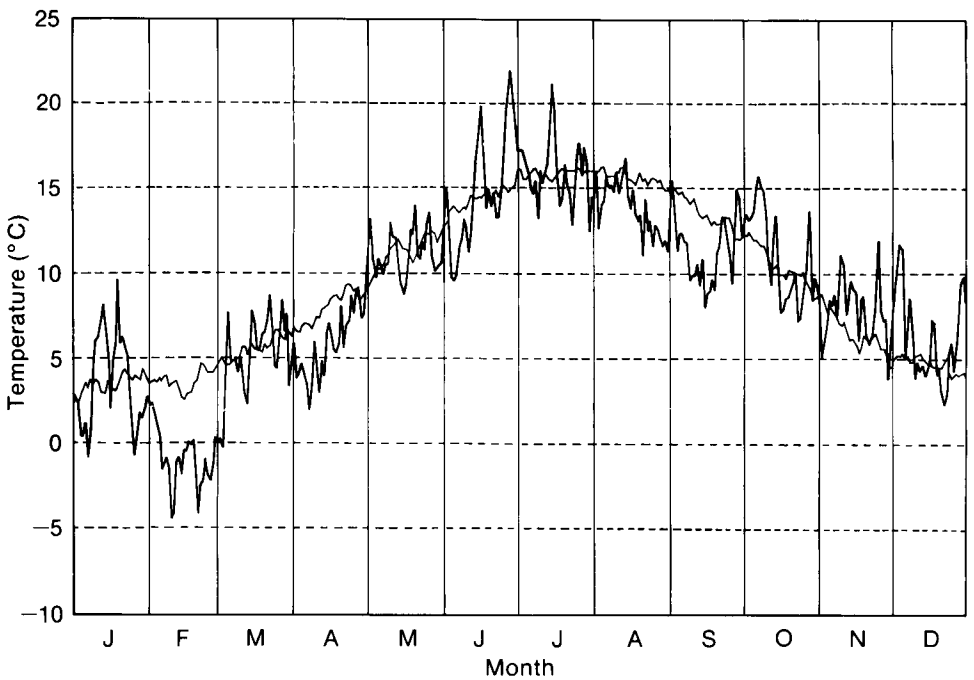

Figure 1. Daily Central England Temperature for 1986, and the 1951–80 normals.

weeks, is increasingly recognized (e.g. Barnston and Livezey 1987). Although the shortest-term fluctuations can be predicted a few days in advance by using atmospheric general circulation models provided with timely data well distributed over the globe, prediction of the variations on time-scales of weeks and months requires a better understanding and representation of the physics of the world's climate system, including ocean–atmosphere interaction. Statistical techniques can also be used with some limited success to make forecasts for the United Kingdom for a month ahead if the methods used take account of conditions world-wide (Folland, Woodcock and Varah 1986).

Fig. 2 (from Folland and Woodcock 1986) contrasts the atmospheric circulation in the two very different summers of 1983 and 1985. The maps show the tracks of the strongest westerlies at 500 mb for 5-day periods. These tracks are closely linked with the tracks of depressions giving wet and windy weather. In 1983 the tracks bypassed Britain to the north, and the country experienced a very warm and dry summer; in 1985 the tracks crossed the country and the summer was cool and wet. Scotland was especially wet because the wettest conditions are generally slightly north of the axis of the strongest upper westerlies. The summer of 1985 had more day-to-day variability than that of 1983, in association with passing troughs and ridges; 1983 was settled and anticyclonic. This, and the previous illustration,

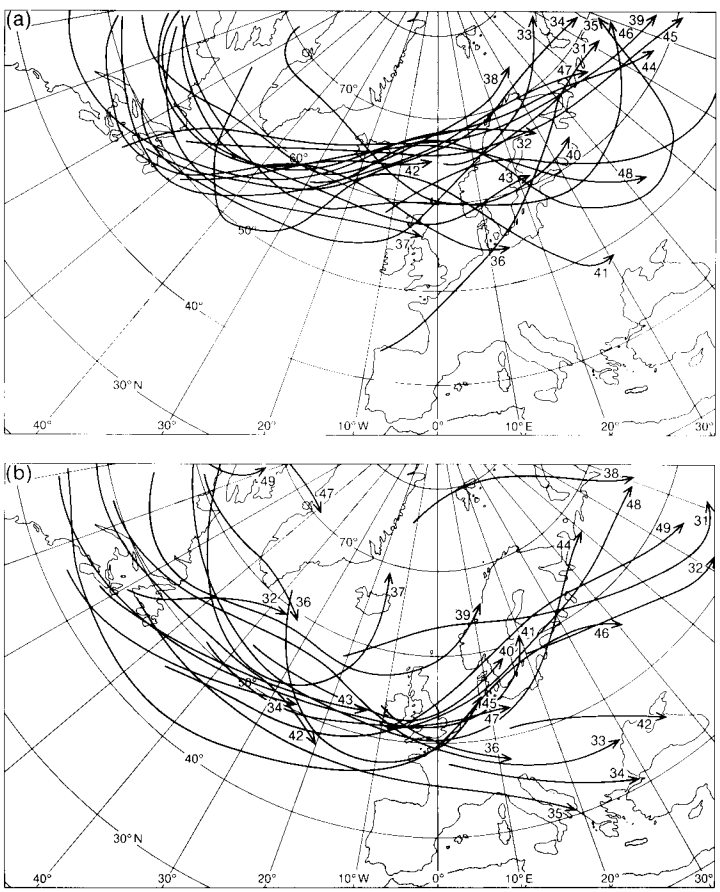

Figure 2. Position of 5-day (pentad) mean maximum wind speed (> 50 kn) at 500 mb during June, July and August for (a) 1983 and (b) 1985. The arrows indicate the direction of the mean flow and the figures give the pentad number (e.g. 41 refers to the 41st 5-day period into the year). (From Folland and Woodcock 1986.)

shows that local or regional short-term climatic variability includes an erratic tendency to longer spells of more or less persistently abnormal atmospheric conditions of similar character. Research needs to be directed at understanding these longer spells, because a persistent tendency for a given type of long spell to repeat at a given season more frequently than before for an extended period would constitute one prominent type of regional climatic change.

3. Long-term variability

If short-term variations need to be studied with a world-wide perspective, then the same is clearly true of longer-term variability because of the greater involvement of the slowly varying parts of the world's climatic system, especially the oceans. The long-term variations manifest themselves as changes in mean values and changes in variability.

3.1 *Changes in mean temperature, precipitation and circulation*

The reality of long-term temperature variations during the past 150 years on a scale as large as the globe itself has now been established beyond doubt. Figs 3(a) and 3(b) show smoothed changes of northern and southern hemisphere sea surface temperatures and land surface air temperatures (relative to a 1951–80 standard) since the mid-nineteenth century (see also Folland *et al.* 1984, Jones *et al.* 1986, Jones, Raper and Wigley 1986). Details in the nineteenth century are still disputed, but the warming for both land and ocean between about 1910 and the 1940s is well established and really was world-wide in that it occurred to a greater or lesser extent everywhere. A subsequent temporary cooling affected the northern hemisphere from about 1945 to 1970 over land and from about 1955 to 1975 over the ocean.

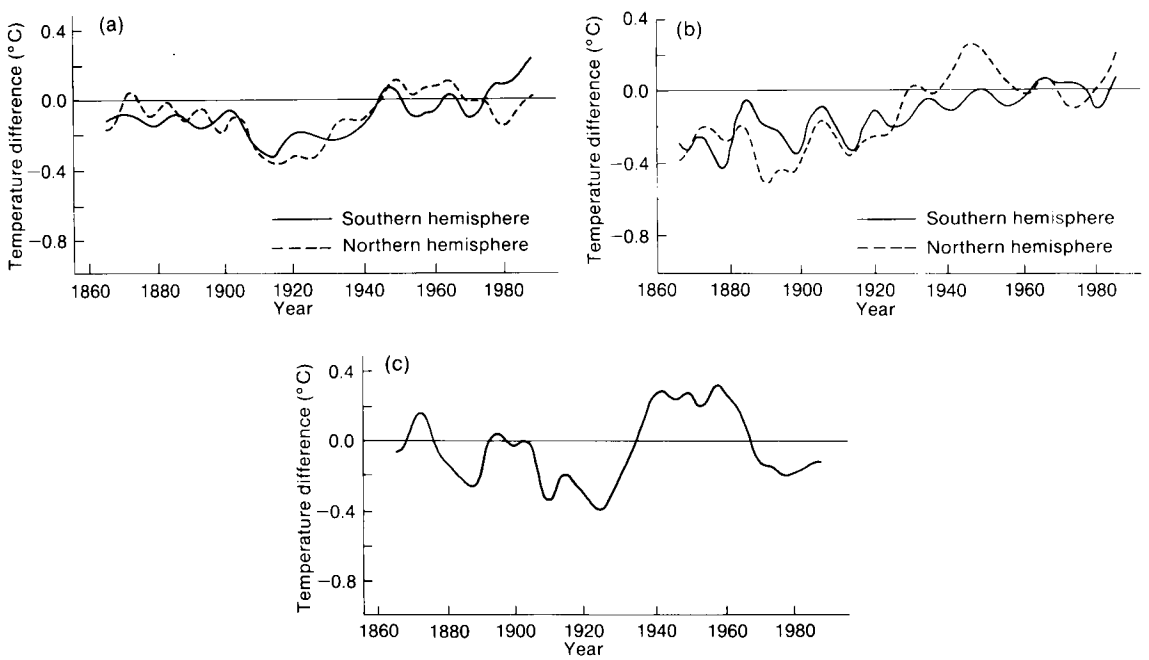

Figure 3. (a) Hemispheric sea surface temperature difference for 1856–1987 relative to 1951–80. (b) Hemispheric land surface air temperature difference for 1856–1984 relative to 1951–80. (From data supplied by P.D. Jones, University of East Anglia.) (c) Sea surface temperature difference for 1856–1987 relative to 1951–80 for the Atlantic Ocean north of 35° N. All were plotted at the end date of a 10-year smoothing filter.

The very recent global warming has been most noticeable in the southern hemisphere and parts of the tropics. Instrumental corrections (which reduce the amplitude of the measured variations) have been applied to sea surface temperatures observed up to the Second World War to compensate for the predominant use of uninsulated buckets to measure sea temperature up to that time. The long-term changes in sea surface temperature averaged over the extratropical North Atlantic have also been marked (Fig. 3(c)). These changes should be sufficient, according to energy-budget considerations, to give rise to significant changes in atmospheric circulation whose character cannot, however, thereby be deduced at present from a knowledge of the sea surface temperature changes alone. Nevertheless, changes in atmospheric circulation on these longer time-scales have indeed been observed. Fig. 4 shows that, in winter, the period 1901–30 had much stronger westerlies over the North Atlantic than did the period 1951–70. As a result, there were few cold winters in the United Kingdom between 1901 and 1930 and, at least in the west, Britain was windier then (Palutikof *et al.* 1987). What is not yet clear is the extent to which the atmospheric circulation changes caused, or were caused by, the oceanic temperature changes. The question needs to be investigated with the aid of numerical models with realistic representation of the physics of ocean–atmosphere interaction.

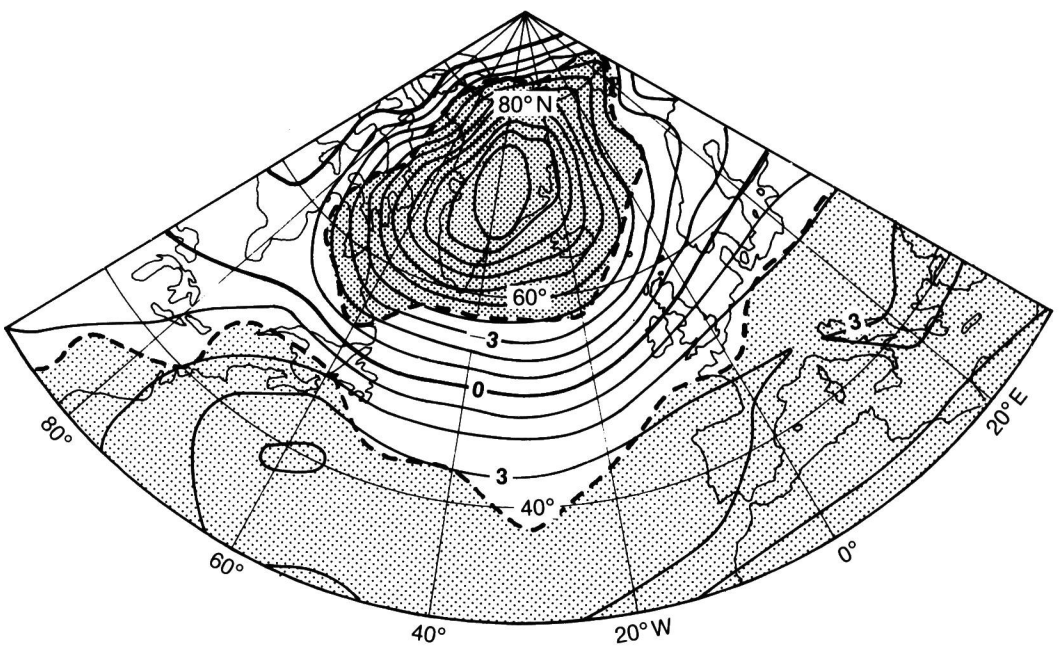

Figure 4. Mean-sea-level pressure difference (mb) for January 1901–30 relative to January 1951–70. Areas of 5% significant difference obtained using a Student's *t*-test (approximate assessment) are shaded: heavy shading, 1901–30 lower; light shading, 1901–30 higher.

A cooling has been observed in north-western Britain since about 1960, especially in northern Scotland (Fig. 5). A reason for this change appears to be the simultaneous decline in sea surface temperatures in the middle-latitude North Atlantic (Fig. 3(c) and Fig. 6) over which the air has often passed to reach the above regions. The linear trend-regression in Fig. 5 is included to illustrate the cooling. The trend correlation of −0.35 is just statistically different from zero at the 95% level of confidence but, in the absence of a full understanding of the physical mechanisms involved, it is not possible to estimate future trends.

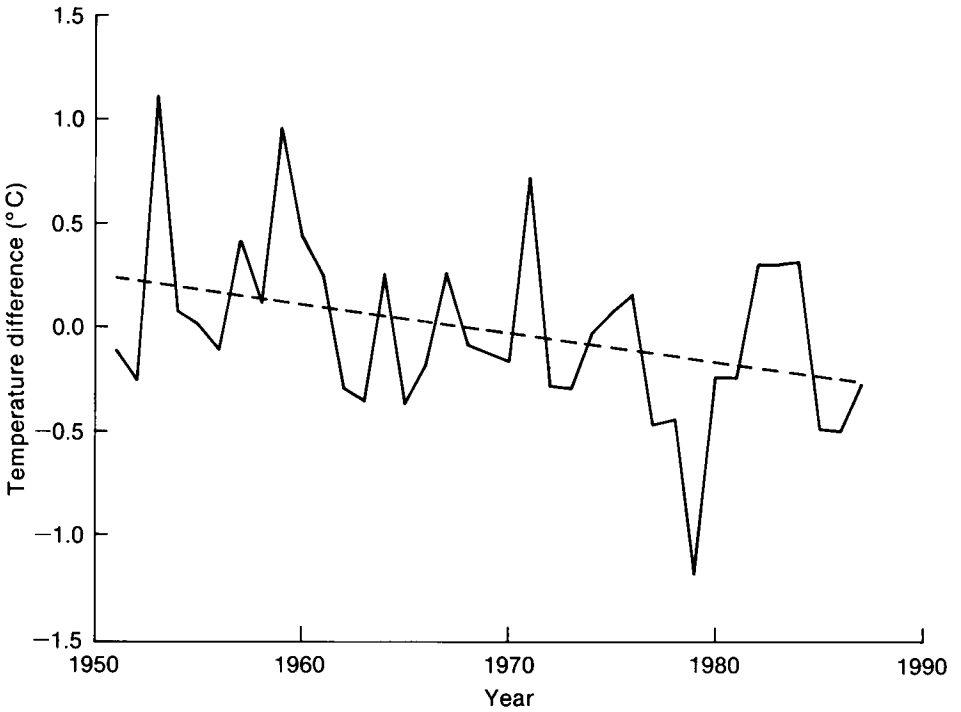

Figure 5. Annual mean temperature difference for northern Scotland, 1951–87 relative to 1951–80. The dashed line is a linear trend-regression.

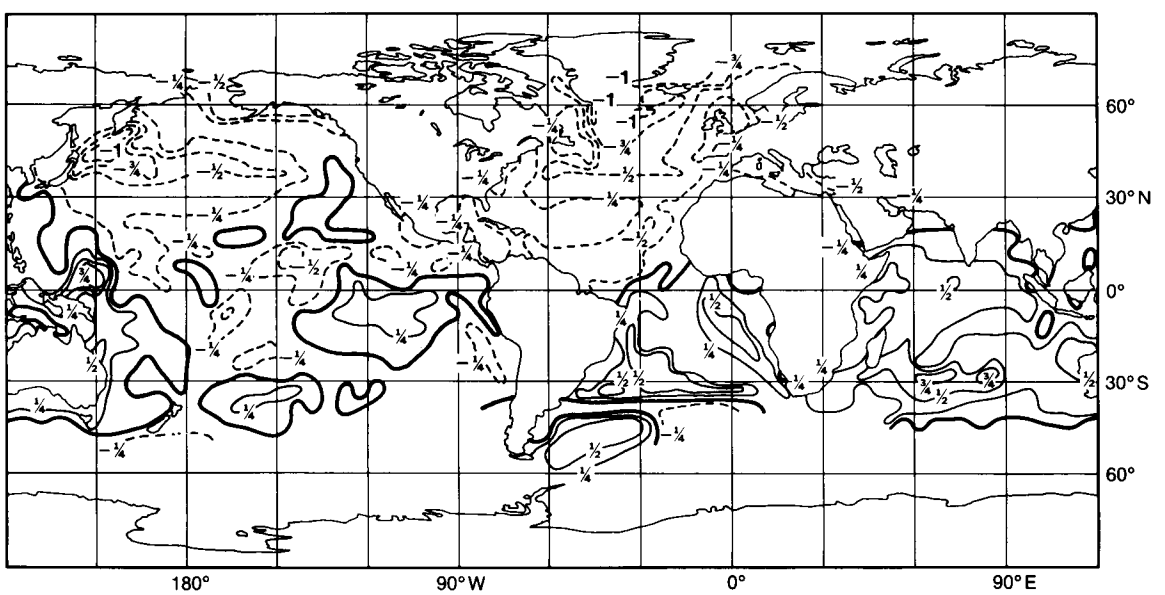

Figure 6. Mean sea surface temperature difference (°C) for 1971–1987 relative to 1951–60.

The warming of the southern hemisphere oceans, relative to those in the northern hemisphere in recent decades (evident in Fig. 3(a) and Fig. 6), appears to be associated with the recent droughts in sub-Saharan Africa (Folland, Palmer and Parker 1986). Effects of this pattern on weather in the United Kingdom are less certain, but the changes have coincided with a recent longer-term tendency to dry summers (Fig. 7). The summers of 1985–87 did not reverse these indications of generally drier summer conditions. The extreme summer drought of 1976 and the very dry summer of 1983 were two of the three driest summers in the record of over 200 years; 1984 was also very dry and gave rise to a brief drought emergency in England and Wales. It must be stressed that there is no indication of any regular variation in the summer rainfall series. The same remark applies to Fig. 8 which shows the great warmth of October in central England in recent decades, in comparison with the whole period from 1659 to about 1940. Before predictions of long-term variations can be attempted, their physical causes need to be investigated using a combination of observational and numerical modelling techniques.

3.2 *Changes in variability*

The examples of long-term variability presented so far have only been discussed in terms of shifts in the average. However, long-term climatic fluctuations may also involve changes in variability about the average. Fig. 9 illustrates changes in the interannual variability of monthly Central England Temperature for selected months of the year. In the early twentieth century, when winter westerlies predominated (Fig. 4) and cold winters were rarer, the standard deviation (scatter) of January Central England Temperature was low. At the same time the skewness of the January values was near zero, i.e. the January mean temperatures were almost normally distributed about the mean. Recently, the standard deviation has increased and the skewness has become rather negative, indicating more very cold Januaries than very mild ones. December and February show similar changes to a lesser extent. A recent increase in positive skewness in July reflects an increased tendency to occasional very hot months (e.g. 1976, 1983); a similar feature is shown by August but not by June. The recently increased likelihood of warm summers is consistent with the tendency to drier summers shown in Fig. 7.

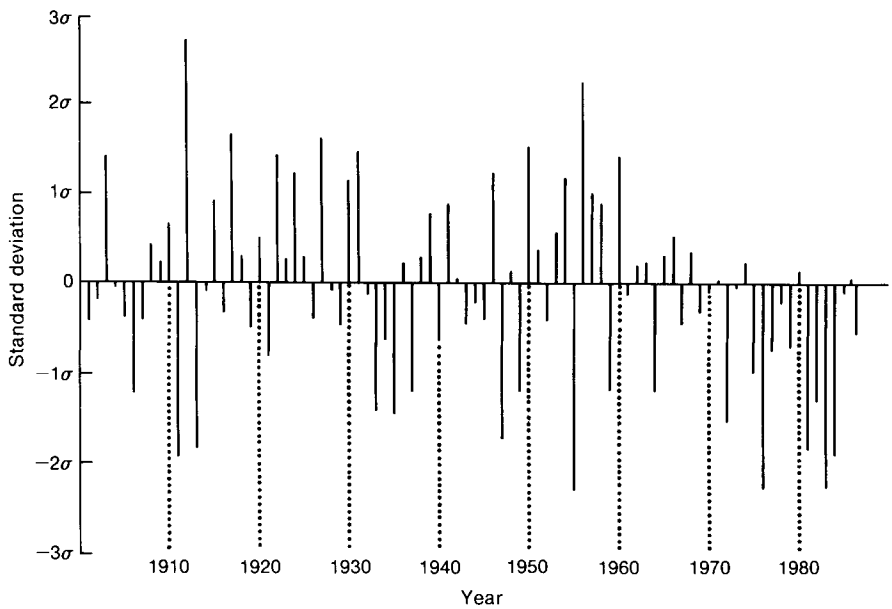

Figure 7. Standardized July and August total rainfall for England and Wales, 1901–87, based on the period 1901–80.

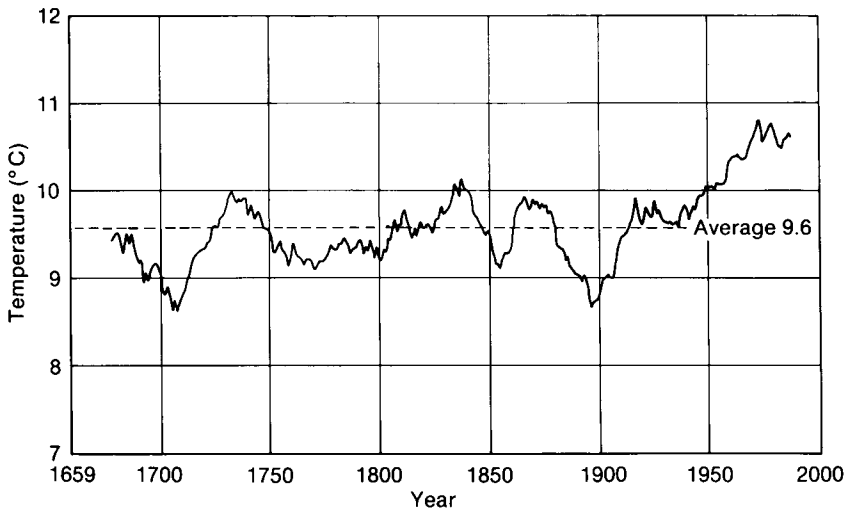

Figure 8. 20-year running mean monthly Central England Temperature for October, 1659–1987.

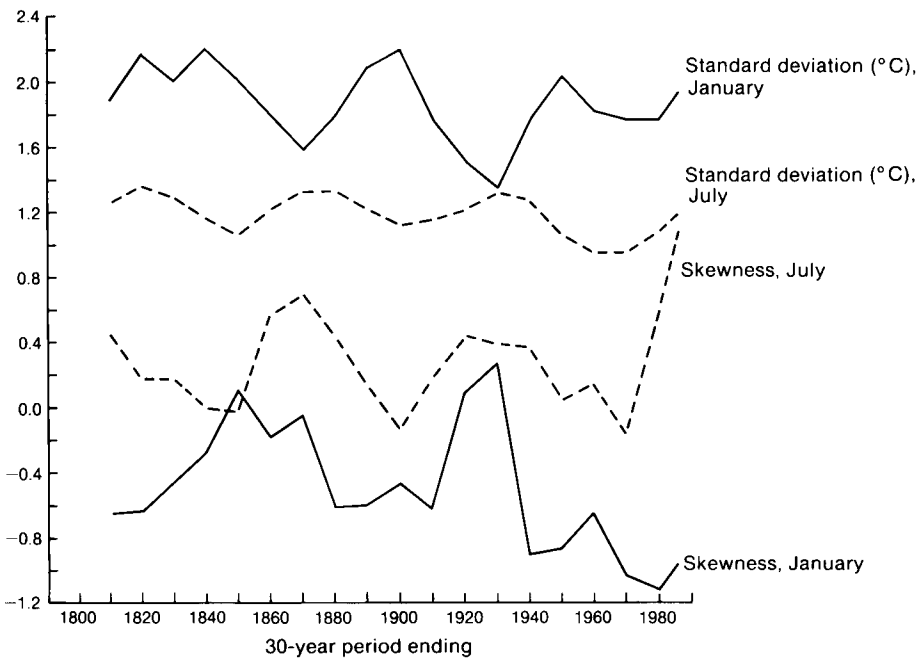

Figure 9. Variability of January and July monthly Central England Temperature from 1781–1810 to 1956–85.

A change in the incidence of perceived 'extremes' need not of course imply a change in short-term variability, because a change in the average of a given sign is likely to increase the frequency of extremes of that sign, and vice versa. Thus the general warming of October in the United Kingdom during this century, and especially since 1940 (Fig. 8), has been associated with an increased number of very mild Octobers and a reduced number of very cold ones.

4. Prediction

For periods of up to a month into the future, statistically based prediction for the United Kingdom has shown limited but definite skill (Folland, Woodcock and Varah 1986). For the tropics, rather longer time-scale predictions of Sahel seasonal (June to October) mean rainfall based on developments of the work of Folland, Palmer and Parker (1986) have been somewhat more successful (Parker *et al.* 1988), though the methods used have not yet had to stand the test of time. Hastenrath *et al.* (1984) have also provided good evidence for potential predictability, months in advance, of rainfall in the wet season in north-eastern Brazil; and evidence of potential skill of the same order has recently been demonstrated for the Indian monsoon by Hastenrath (1987). All these predictions have been strongly guided by an understanding of the physical processes at work, and recently by the use of numerical models to make detailed studies of those processes. Numerical models forced with observed sea surface temperatures have now been used to simulate Sahel monthly and seasonal rainfall in specific past years, with encouraging preliminary results (Owen and Folland 1988).

A different approach to estimating future climate is the use of the 'actuarial' method; that is the use of statistics of the past and present climate to estimate the probabilities of future events, often expressed in terms of 'return period' or the average time interval between events of magnitude on or beyond some threshold. Strictly speaking, however, this is not prediction, and it does not require in-depth physical understanding of the climate system.

The remaining approach to the estimation of future longer-term climatic conditions is via numerical modelling of the physical processes underlying climatic change and variability. Estimation of long-term climatic variations by this means therefore demands the simulation of the oceans and cryosphere as well as the atmosphere. Also, assessments are required of uncertain future man-made inputs such as increasing atmospheric carbon dioxide and other greenhouse gases. Other possible future influences, such as changes in solar radiation, the occurrence of major volcanic eruptions or changes of the frequency and intensity of El Niño type warmings, which eventually influence much of the world (Pan and Oort 1983), are further sources of uncertainty. At present the use of numerical modelling in longer-term climate studies is mainly limited to determining the equilibrium response of the atmosphere to an a priori specification of a physical change in the climate system, e.g. a doubling of atmospheric carbon dioxide or a change of the solar constant by a few per cent. Results are very sensitive to the design features of the models themselves; the globally averaged warming for a doubling of carbon dioxide deduced for various models ranges between 2 and 5 °C. The models differ to an even greater extent in some of their indications of the regional and local climatic responses to a carbon dioxide increase, partly because they do not agree in their simulation of the present regional climate or on how regional atmospheric circulation patterns will change. However, there are some qualitative agreements such as the enhancement of warming near the poles in winter, earlier spring snowmelt, and increased annual mean run-off in high latitudes. Much further research and development is required, therefore, before the models realize anything like their full potential (Wilson and Mitchell 1987).

5. Conclusion

The increasing evidence of man's influence on the global climate indicates a clear need to intensify research into climatic variability, using a combination of observational and numerical modelling studies. Local or regional climatic variability cannot be understood in isolation; a global context is essential, and it is essential to take the oceans into account when studying atmospheric changes on time-scales longer than a few weeks. Understanding the world's climatic system, with its many complex interactions and feedbacks, is the *sine qua non* of climatic prediction, and is one of the most complex tasks in current scientific endeavour.

References

Barnston, A.G. and Livezey, R.E. 1987 Classification, seasonality and persistence of low-frequency atmospheric circulation patterns. *Mon Weather Rev*, **115**, 1083–1126.

Folland, C.K. and Woodcock, A. 1986 Experimental monthly long-range forecasts for the United Kingdom. Part I. Description of the forecasting system. *Meteorol Mag*, **115**, 301–318.

Folland, C.K., Palmer, T.N. and Parker, D.E. 1986 Sahel rainfall and worldwide sea temperatures, 1901–85. *Nature*, **320**, 602–607.

Folland, C.K., Parker, D.E. and Kates, F.E. 1984 Worldwide marine temperature fluctuations 1856–1981. *Nature*, **310**, 670–673.

Folland, C.K., Woodcock, A. and Varah, L.D. 1986 Experimental monthly long-range forecasts for the United Kingdom. Part III. Skill of the monthly forecasts. *Meteorol Mag*, **115**, 377–395.

Hastenrath, S. 1987 On the prediction of India monsoon rainfall anomalies. *J Clim Appl Meteorol*, **26**, 847–857.

Hastenrath, S., Wu, M-C. and Chu, P-S. 1984 Towards the monitoring and prediction of north-east Brazil droughts. *Q J R Meteorol Soc*, **110**, 411–425.

Jones, D.E. 1987 Daily Central England Temperature: recently constructed series. *Weather*, **42**, 130–133.

Jones, P.D., Raper, S.C.B. and Wigley, T.M.L. 1986 Southern hemisphere surface air temperature variations: 1851–1984. *J Clim Appl Meteorol*, **25**, 1213–1230.

Jones, P.D., Raper, S.C.B., Bradley, R.S., Diaz, H.F., Kelly, P.M. and Wigley, T.M.L. 1986 Northern hemisphere surface air temperature variations: 1851–1984. *J Clim Appl Meteorol*, **25**, 161–179.

Manley, G. 1974 Central England Temperatures: monthly means 1659 to 1973. *Q J R Meteorol Soc*, **100**, 389–405.

Owen, J.A. and Folland, C.K. 1988 Modelling the influence of sea surface temperatures on tropical rainfall. *In* S. Gregory (ed); Recent climatic change — a regional approach. London, Belhaven Press.

Palutikov, J.P., Kelly, P.M., Davies, T.D. and Halliday, J.A. 1987 Impacts of spatial and temporal windspeed variability on wind energy output. *J Clim Appl Meteorol*, **26**, 1124–1133.

Pan, Y.H. and Oort, A.H. 1983 Global climate variations connected with surface temperature anomalies in the eastern equatorial Pacific Ocean for the 1958–73 period. *Mon Weather Rev*, **111**, 1244–1258.

Parker, D.E., Folland, C.K. and Ward, M.N. 1988 Sea surface temperature anomaly patterns and prediction of seasonal rainfall in the Sahel region of Africa. *In* S. Gregory (ed); Recent climatic change — a regional approach. London, Belhaven Press.

Wilson, C.A. and Mitchell, J.F.B. 1987 A doubled CO_2 climate sensitivity experiment with a global climate model including a simple ocean. *J Geophys Res*, **92**, 13 315–13 343.

551.576.4:551.524.72:551.507.362.2

Cloud-top temperature/height: A high-resolution imagery product from AVHRR data

R.W. Saunders

Meteorological Office Unit, Robert Hooke Institute for Atmospheric Research, Clarendon Laboratory, Oxford

Summary

A scheme for deriving accurate cloud-top temperatures and cloud-top heights from NOAA Advanced Very High Resolution Radiometer (AVHRR) data is described. To illustrate the products derived using this scheme three case-studies were chosen, one with deep convective cloud along the east coast of England on 14 April 1985, one with a marked cold front across the British Isles on 3 September 1986 and one with patchy fog over southern England on 23 October 1983.

1. Introduction

One of the principal meteorological variables of interest to aviation forecasters is the height and/or temperature of the cloud/fog tops within their area of responsibility. This quantity is not easy to determine accurately from surface observations and can only be inferred at a few points, twice a day, from radiosonde temperature and humidity profiles.

Satellite images, however, offer the possibility of obtaining reasonably accurate estimates of cloud-top height over a large area. Meteosat imagery is currently used operationally for determining cloud-top heights by computing a cloud-top height image product which is then disseminated to users three times a day using the WEFAX transmissions (Bowen 1982). This has proved to be a useful product for civil airline pilots who use it to help them plan their routes. The advantage that Meteosat has, is that the data are available every half hour and so the development of a rapidly changing cloud system can be monitored. The disadvantage of the Meteosat product is the relatively low horizontal resolution of individual radiance measurements over north-western Europe (≈ 9 km $\times$ 6 km). In contrast, data from the Advanced Very High Resolution Radiometer (AVHRR) on the NOAA polar-orbiting satellites can give a cloud-top height product with a horizontal resolution as high as 1.1 km, four times a day (assuming a two-satellite system which is normally the case). One way of making use of the advantages of both sampling systems would be to 'calibrate' the Meteosat cloud-top heights using the AVHRR product.

A cloud-top temperature/height product has a number of applications. For aviation forecasts the current location and accurate cloud-top height of significant convective and frontal cloud systems over the area of interest would be valuable information to take into account while preparing the local area and route forecasts. The temperature of fog tops is also a useful parameter for estimating how quickly fog might clear at an airfield or along a stretch of motorway.

This paper describes a scheme for deriving accurate cloud-top temperatures and heights from AVHRR data and some examples of cloud-top products produced by such a scheme are presented. Where possible the product is validated with coincident radiosonde profiles. Work is now in progress at the Meteorological Office to make possible the dissemination of such products to forecast offices in the United Kingdom within an hour of receipt of the data.

2. Determination of cloud-top temperature and height from AVHRR data

This section explains the various steps required to retrieve a cloud-top temperature and height product from the raw AVHRR data received from the spacecraft. Fig. 1 shows the principal operations in the processing scheme which are described in more detail below.

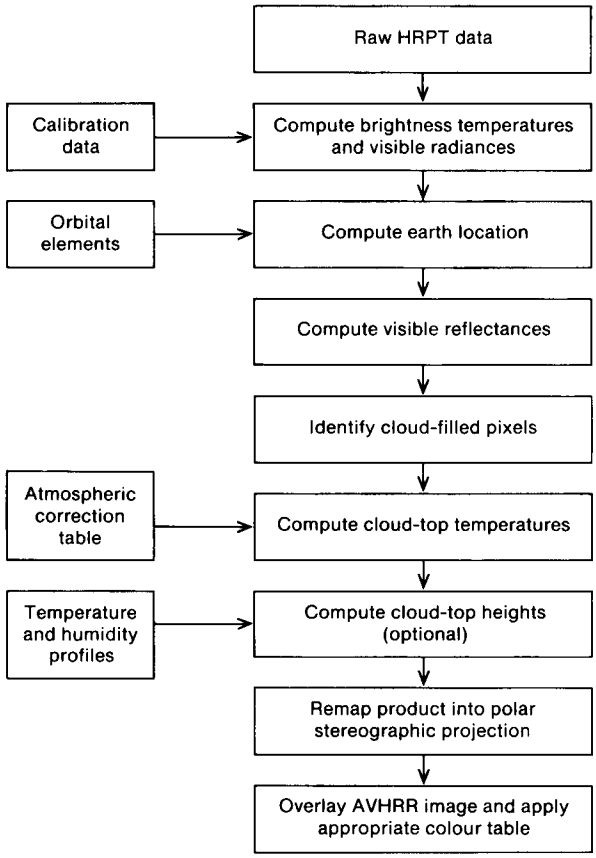

Figure 1. Flow diagram showing how the raw HRPT data received from the spacecraft are processed to give a cloud-top temperature or height image.

2.1 *Preprocessing of AVHRR data*

Data from the NOAA satellites are collected by the ground station at Lasham, in Hampshire, which provides the Meteorological Office with most of the satellite data which are used operationally. The digital AVHRR data are received from the NOAA spacecraft as part of the High Resolution Picture Transmission (HRPT) data stream. The basic processing scheme for determining cloud-top height from the raw HRPT data is shown in Fig. 1 and is part of a more general AVHRR processing software package called APOLLO (AVHRR processing over land cloud and ocean) developed for research purposes in the Meteorological Office (Saunders and Pescod 1988).

The initial processing of the AVHRR data follows the same steps as those outlined in Pescod *et al.* (1986) to derive a sea surface temperature product and so the interested reader is referred to section 2 of that paper for more details. However, one major difference is in the use made of the results from the cloud analysis. This cloud analysis step actually classifies a pixel as cloud-free, partly cloudy or cloud-filled in one operation. The details of this analysis have been described by Saunders and Kriebel (1988) who give some examples of cloud-free and cloud-filled pixels that were identified by the analysis for the scheme described here. Instead of using the pixels identified as cloud-free (for determining surface parameters), only cloud-filled pixels are used here for determining cloud-top temperature.

2.2 *Determination of cloud-top temperature*

The next step is to compute a representative cloud-top temperature from the pixels identified as cloud-filled. To explain the basis of this method the various contributions to the measured satellite radiance, shown in Fig. 2, are considered. The radiance, I_{11}, measured by a satellite radiometer above the atmosphere at a wavelength of 11 μm (corresponding to channel 4 of the AVHRR) where aerosol and cloud scattering effects and reflection of solar and downwelling atmospheric radiation by the cloud top are neglected, is given by

$$I_{11}(\theta,\phi,\Psi) = \epsilon_c(\theta,\phi)B(T_c)\tau^H_{h_c}(\Psi,\theta) + \int_{h_c}^{H} B(T(h))\frac{\partial \tau^H_h(\Psi,\theta)}{\partial h}\,dh +$$

$$+ (1 - \epsilon_c(\theta,\phi))I_s(\Psi,\theta,\phi)\tau^H_{h_c}(\Psi,\theta) \quad \ldots\ \ldots\ \ldots\ \ldots\ \ldots\ \ldots \quad (1)$$

where ϵ_c is the emissivity of the cloud, T_c is the cloud-top temperature, $\tau^{h_2}_{h_1}$ is the atmospheric transmission from height h_1 to h_2 (H is the top of the atmosphere and h_c is the height of the top of the cloud), $B(T)$ is the Planck function for a temperature, T, at a wavelength of 11 μm and I_s is the upwelling radiance entering the cloud base; θ and ϕ represent satellite zenith and azimuth angles from the cloud top and Ψ the atmospheric state (e.g. water vapour amount, pressure, temperature, etc.).

The first term normally represents the radiation emitted by the cloud top, as shown in Fig. 2, and will generally be the dominant contribution to the measured radiance at a wavelength of 11 μm where the atmospheric absorption is small. The second term represents the upwelling radiation emitted by the atmosphere between the cloud top and the top of the atmosphere. This term will be small except over low

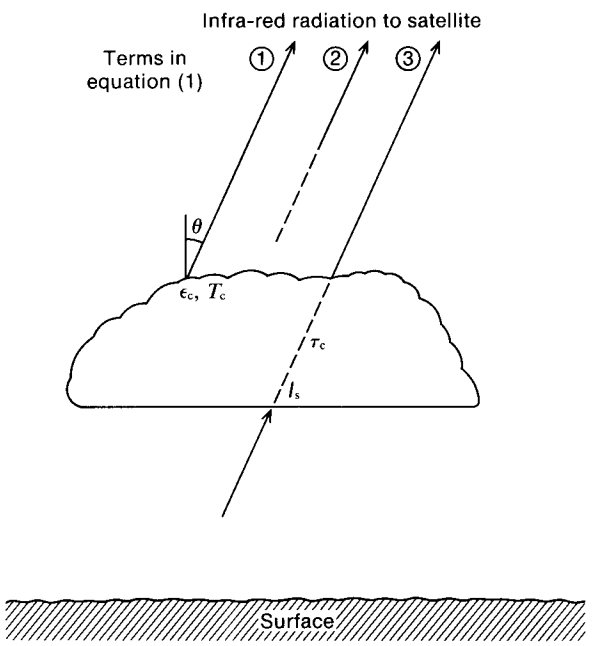

Figure 2. Schematic diagram showing the three different components of infra-red radiation over a cloud top which are detected by a satellite sensor. See text for explanation of symbols.

cloud in warm, moist, tropical atmospheres. The third term represents the upwelling surface radiation after attenuation by the cloud and atmosphere. For thick stratus or cumuliform cloud nearly all the surface radiation is absorbed by the cloud and this term becomes negligible. However, for thin cirrus cloud, typically 50% of the upwelling radiation from below will be transmitted and contribute to the overall measured radiance I_{11}. This effect complicates the measurement of cloud-top temperature from a single infra-red radiance measurement in one channel.

For this study, to simplify matters, a test was devised to identify thin cirrus cloud by the temperature difference obtained between channels 4 and 5 when semi-transparent cloud is in the field of view. The basis for this test is described in Saunders and Kriebel (1988). Cloud-top temperatures were not computed from pixels which were identified as containing semi-transparent cloud; hence term 3 of equation (1) can be neglected for this study. The assumption that the radiation measured by the satellite emanates from the cloud top (i.e. $\epsilon_c = 1$) was checked by Kriebel *et al.* (1983) by making coincident satellite and airborne lidar measurements of cloud-top heights. For optically thick high cloud they reported a mean difference of 0.4 km (equivalent to ≈ 3 K). Over fog some comparisons of aircraft, radiosonde and satellite measurements made by Findlater *et al.* (1988) indicated a mean difference of about 1 K in fog-top temperature between the different measurements. For clouds which are optically thick (i.e. $\epsilon_c = 1$) equation (1) simplifies to

$$I_{11} = \tau^H_{h_c}(\Psi,\theta)B(T_c) + \int_{h_c}^{H} B(T(h))\frac{\partial \tau^H_h(\Psi,\theta)}{\partial h}\,dh\,. \qquad \ldots\ \ldots\ \ldots\ \ldots\ (2)$$

To determine T_c from I_{11} we only need to know the transmission and emission of the atmosphere between the cloud top and the satellite sensor. The atmospheric emission is generally small for channel 4 of AVHRR centred at a wavelength of 10.7 μm. The atmospheric transmission/emission between 10 and 11.8μm for a range of atmospheric conditions was computed using a line by line atmospheric transmission model (Edwards 1987). Two representative sets of radiosonde profiles of temperature and humidity over the British Isles for January and July were used to compute the atmospheric transmittances and emitted radiances. Given T_c, values for I_{11} were computed from the model using equation (2). These simulated radiance values for I_{11} showed that, as the atmospheric correction term is small at mid-latitudes and normally reduces the measured cloud-top temperature T_c, it can be expressed as a correction factor, ΔT, which allows the cloud-top temperature to be computed simply from the measured 11 μm brightness temperature T_{11} (i.e. equivalent black-body temperature integrated over the channel response) by using the expression

$$T_c = T_{11} + \Delta T(T_{11},\theta).$$

This enables T_c to be computed quickly from T_{11} for each pixel, reducing the overall computation time. A table of ΔT values for a range of values for T_{11} and satellite zenith angles θ is listed in Table I. They were computed by averaging the computed ΔT values for January and July. The differences between the values for the two months were small (e.g. ≈ 0.3 K for T_{11} of 270 K and sec θ of 2). ΔT increases for higher values of T_{11} because T_{11} is correlated with the total column water amount. Also ΔT increases with increasing values of θ due to the longer atmospheric path lengths between the cloud top and satellite sensor. For cloud tops with temperatures below 230 K the atmospheric absorption/emission contribution becomes negligible.

For optically thick cloud, one main uncertainty in this approach will be how representative the precomputed ΔT values are of the actual atmospheric state at the time of the satellite measurement. This uncertainty could be as much as 0.5 K for a low cloud top overlaid with a warm, moist atmosphere, but is negligible for high cloud tops. It could be reduced by using a ΔT value calculated from either a

Table I. *Atmospheric correction factors, ΔT, in degrees K to be added to the measured AVHRR channel 4 brightness temperatures, T_{11}, to retrieve cloud-top temperature, where θ is the satellite zenith angle from the cloud top. These factors are for an annual mean atmosphere (i.e. average of January and July factors) appropriate to conditions over the British Isles.*

	Sec θ values				
T_{11} (K)	1.0	1.25	1.50	1.75	2.0
220	0.0	0.0	0.0	0.0	0.0
225	0.1	0.1	0.1	0.1	0.1
230	0.1	0.1	0.2	0.2	0.2
235	0.2	0.2	0.2	0.3	0.3
240	0.2	0.3	0.3	0.4	0.4
245	0.3	0.3	0.4	0.5	0.5
250	0.3	0.4	0.5	0.6	0.6
255	0.4	0.5	0.6	0.7	0.7
260	0.5	0.6	0.7	0.8	0.9
265	0.6	0.7	0.9	1.0	1.1
270	0.8	0.9	1.1	1.2	1.3
275	0.9	1.0	1.2	1.3	1.5
280	1.2	1.4	1.6	1.7	1.9
285	1.5	1.7	2.0	2.1	2.3
290	1.9	2.2	2.5	2.6	2.8

coincident sounder profile (i.e. from the TIROS Operational Vertical Sounder (TOVS)) or a model forecast profile — the latter being easier to use.

In the future this method could be extended to allow for semi-transparent cloud. There have been a number of methods developed to determine the cloud-top temperature of semi-transparent cloud from Meteosat data by using a combination of the window channel (10.5–12.5 μm) and the water vapour channel (5.7–7.1 μm) radiances (e.g. Szejwach 1982). However, AVHRR has no water vapour channel, so these methods for determining an accurate cloud-top temperature for semi-transparent cloud cannot be used. Inoue (1985) has developed a method using channels 4 and 5 of the AVHRR (corresponding to wavelengths of 10.3–11.3 μm and 11.5–12.5 μm respectively) to determine temperature and effective emissivities of semi-transparent cloud. However, it relies on part of the cirrus cloud being optically thick, which is often not the case.

The advantage of AVHRR data as compared with Meteosat data is that the smaller field of view of the former at the cloud top ensures that many cloud-filled pixels can be identified in the image. This, together with the more reliable ($\approx$ 0.2 K) calibration of the AVHRR radiometer, allows a more accurate radiative cloud-top temperature at a higher spatial resolution to be obtained.

The cloud-top temperature is derived from cloud-filled pixels as described above and displayed in the format illustrated by the example in Fig. 3(a). In some situations, for instance over low stratus cloud or fog, the forecaster would be more interested in the cloud-top temperature than cloud-top height.

2.3 *Determination of cloud-top height*

The cloud-top temperature can now be converted to a height using a representative temperature and humidity profile. The simplest solution would be to use a climatological mean profile for the month of interest over north-western Europe. However, as Kriebel *et al.* (1983) point out, this can lead to errors of 1.8 km in the derived cloud-top height as the climatological profile is often not representative of the

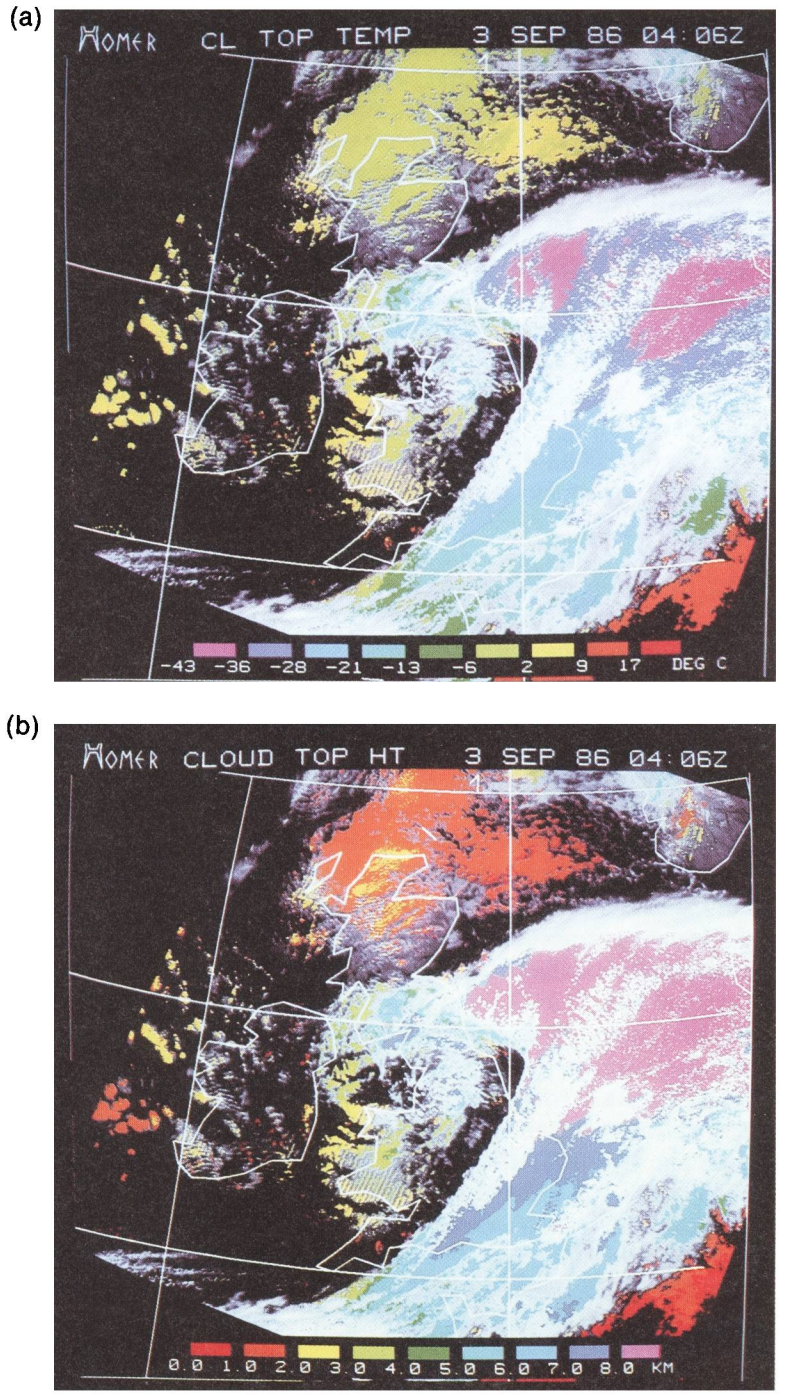

Figure 3. (a) Cloud-top temperature (°C) and (b) height (km) image over the British Isles for 3 September 1986 at 0406 GMT. The linear features over the cloud in south-west Wales are artefacts caused by the noise in the 3.7 μm channel used to identify cloud-filled pixels.

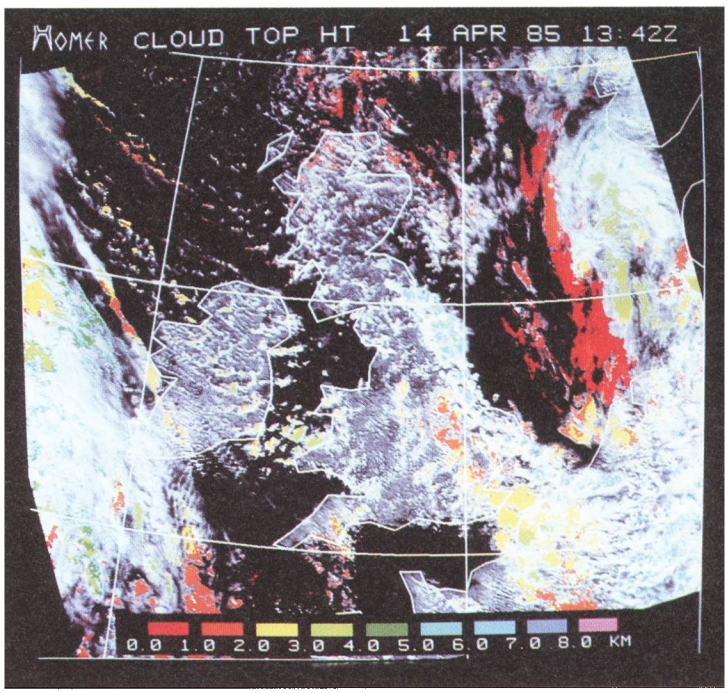

Figure 4. Cloud-top height (km) image for 14 April 1985 at 1342 GMT.

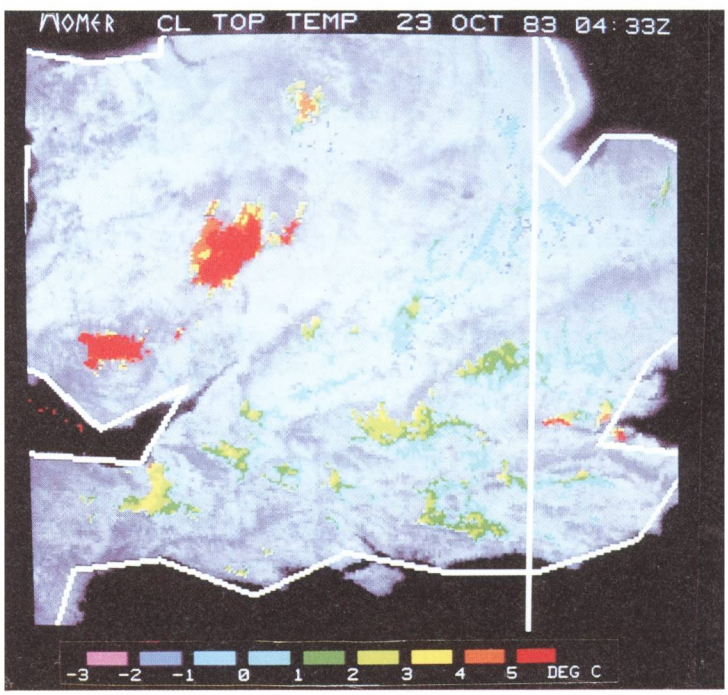

Figure 5. Cloud-top temperature (°C) image for 23 October 1983 at 0433 GMT.

actual atmospheric conditions. For this study, radiosonde profiles closest in time to the satellite overpass were used to relate cloud-top temperature to height and four stations were taken to cover the local area — Lerwick, Hemsby, Camborne and Valentia. The profile from the station nearest to the pixel was taken to be the most representative which was then used to convert cloud-top temperature at a pressure, P, to a height, Z_c, by using the hydrostatic equation given by

$$Z_c = -\frac{R}{gM_a}\int_{P_0}^{P}\frac{T_v(P)}{P}dP$$

where R is the gas constant per mole, g the acceleration due to gravity, M_a the molecular weight of dry air, P_0 the pressure at the surface and T_v the virtual temperature which allows for the water vapour in the column.

In an operational scheme it would be preferable to take the temperature and humidity profiles from a regional forecast model (e.g. a 6-hour forecast from the Meteorological Office fine-mesh model) as the profiles should be more representative of the real atmosphere in areas some distance from the actual radiosonde ascents. The Meteosat cloud-top height product is currently derived using profiles obtained from the ECMWF forecast model.

The cloud-top height is displayed in the form of a conventional AVHRR visible (daytime) or infra-red (night-time) image which is remapped into a polar stereographic projection. The cloud-filled pixels are then overlaid and coloured according to their cloud-top height or temperature. In this way the cloud coverage as well as the cloud-top heights or temperatures can be observed. The white areas are cloud tops which have been identified as not cloud-filled or optically thick, and so no temperature or height is assigned to them.

3. Examples of cloud-top temperature and height products

To illustrate the application of the scheme described above to AVHRR data, three cases were chosen, one with frontal cloud, one with convective cloud and one with patchy fog over southern England.

3.1 *Frontal cloud*

The first case-study was for a night-time overpass of NOAA-9 at 0406 GMT on 3 September 1986 where a marked cold front lay across southern England. This case is discussed in some detail by Browning *et al.* (1987) using radar and Meteosat imagery. A surface analysis at 0400 GMT shows the cold front lying across south-east England at this time. The location of the front was also well correlated with the rainfall distribution measured by the radar network. The centre of the associated depression was analysed as being over the North Sea to the east of Flamborough Head, Humberside.

The AVHRR image shown in Fig. 3(a) clearly shows the temperature of the cloud tops associated with this frontal system and Fig. 3(b) shows the corresponding cloud-top heights. The temperatures were as low as −40 °C at the triple point (56° N, 1° E) corresponding to a cloud-top height above 8 km. Along the line of the cold front the top temperatures are warmer, being in the range −27 to −18 °C (7–8 km) across south-east England. These values are similar to those derived by Meteosat at 0300 GMT (compare with Fig. 3(a) of Browning *et al.* 1987). It was difficult to estimate a cloud-top temperature from the Hemsby midnight ascent as, being in the warm sector, it was saturated most of the way to the tropopause. The Camborne ascent at midnight (see Fig. 5 of Browning *et al.* 1987) clearly shows that the cloud top was around 600 mb, giving a cloud-top temperature of −10 °C in reasonable agreement with the satellite cloud-top temperatures off the Devon coast; these cloud tops would have been over

Camborne at that time. Over northern Scotland the cloud-top temperatures of the stratocumulus cloud are in the range −6 to +2 °C (corresponding to a height range of 1–2 km) measured by the satellite. The midnight Lerwick ascent shows an inversion at about −2 °C so any cloud tops would be expected to be at or below this inversion layer. Note that parts of the frontal cloud in Fig. 3, which are white, are not assigned a cloud-top temperature/height due to the existence of thin cirrus cloud overlaying the thick frontal cloud.

3.2 *Convective cloud*

The second case-study was for a NOAA-9 pass over the British Isles on 14 April 1985 at 1342 GMT. There was a warm front approaching south-western Ireland at this time with the British Isles in a north-westerly airstream, as can be inferred from the orientation of the cumulus cloud over Ireland, England and Wales in Fig. 4. A line of convective cloud aligned along the east coast of Britain had formed by 1200 GMT, as is evident in both the Meteosat and radar displays for this time (see Fig. 19 of Browning *et al.* 1987). The surface reports at 1200 GMT indicated that rain and hail showers had occurred. By 1500 GMT (after the NOAA-9 overpass) this line of convective cloud had increased in cloud-top height, as shown by the Meteosat imagery, and the intensity of precipitation beneath the cloud had increased, as revealed by the radar. By 1800 GMT thunderstorms had been reported all along the east coast. Fig. 4 shows the cloud-top height product for 1342 GMT derived from AVHRR data. The line of convective cloud along the east coast of England shows up clearly with measured cloud-top temperatures down to at least −40 °C. The heights corresponding to these cloud tops go up to 7 km. The Meteosat images (see Fig. 19(b) in Browning *et al.* 1987) also show the cloud-top temperatures to be below −30 °C, but the large pixel size in this case has failed to identify clearly the individual convective turrets evident in Fig. 4. This convective cloud extended well into Belgium and northern France where it was more widespread and with slightly colder cloud tops (some down to −46 °C).

The Hemsby midday ascent shows the air to be potentially unstable with 'parcel tops' expected to be about −46 °C (i.e. about 7 km) and 'absolute tops' a degree or two cooler. This compares with the satellite-derived cloud-top temperatures in the region of Hemsby being colder than −38 °C in places but no cloud tops colder than −46 °C. The clouds were still developing at this time and so would probably be expected to have tops lower than the predicted parcel tops.

Regarding the cumulus clouds across the British Isles, only the largest are assigned a cloud-top temperature or height as they are generally too small to fill a pixel completely. The larger clouds have cloud-top temperatures of around −5 °C which correspond to heights of 2–3 km. The midday ascent from Long Kesh (Northern Ireland) shows a marked inversion layer at 790 mb giving cloud-top temperatures around −8 °C. The thicker parts of the cirrus cloud associated with the approaching warm front to the south-west of Ireland have a cloud-top height in the range 6–7 km.

3.3 *Patchy fog*

The third case-study was for a situation where there was patchy fog over southern England; it has also been studied in some detail by Turner *et al.* (1986). The AVHRR cloud-top temperature product is shown in Fig. 5 at the time of the NOAA-7 overpass on 23 October 1983 at 0433 GMT. A surface analysis at 0500 GMT shows a ridge of high pressure extending westwards across southern England resulting in clear skies. A layer of stratocumulus, associated with a weak cold front across north-west Scotland, covered northern England and most of Ireland. By 0500 GMT many stations over central southern England were reporting shallow fog (i.e. sky still visible) with visibilities down to 30 m reported (see Fig. 1 of Turner *et al.* 1986).

The satellite product shown in Fig. 5 reveals the fog to be patchy in nature over southern England, consistent with the fact that not all the stations were reporting fog. In general the fog appeared to form in

areas associated with the Chilterns and the North Downs, or in flat areas such as the Somerset Levels and the Fens. Most of the fog patches had a fog-top temperature of about 2 °C which was the same as the reported screen temperatures in this region. Over the Fens, fog-top temperatures dropped to about −1 °C which was confirmed by one report of freezing fog just to the north of the Fens at Coningsby. The warmer tops (> 5 °C) over southern Wales and the Severn Valley were assumed to be cloud. This was confirmed over South Wales by an observation of stratocumulus cloud.

4. Discussion and conclusions

The feasibility of deriving a cloud-top temperature or height product from AVHRR data for forecasting purposes is demonstrated for three different meteorological situations. Uncertainties in the atmospheric absorption correction term lead to uncertainties in the computed cloud-top temperature of up to 0.5 K for low cloud/fog but are negligible for high cloud. Uncertainties due to assuming a cloud-top emissivity of 1 are probably greater, but coincident satellite and aircraft measurements suggest errors of only 1 K for low cloud and up to 3 K for high cloud. This level of accuracy is probably sufficient for forecasting purposes. Where possible the AVHRR cloud-top temperature products have been compared with conventional radiosonde or surface observations. For the three cases presented here the AVHRR products were reasonably consistent with the radiosonde measurements. Differences of several degrees could be explained by the differences in both space and time between the satellite measurement and the radiosonde profile. It will be difficult to validate the satellite products to better than a few degrees until coincident satellite and aircraft measurements are made or ascents are available at the same time as the satellite overpass. Reasonable agreement was also obtained between AVHRR cloud-top temperatures and the corresponding values derived from Meteosat-2 reported by Browning *et al.* (1987).

This paper shows a few examples of a cloud-top temperature/height product. The problems of deriving cloud-top temperature from semi-transparent cloud or partially cloud-filled pixels have not been discussed in detail, though several methods to infer cloud-top temperature from these pixels have been developed (e.g. Inoue 1985). The high-resolution infra-red radiation sounder (HIRS), with many more infra-red channels, is also useful for estimating the cloud-top pressure of semi-transparent cloud (Eyre and Menzel 1988). The inclusion of these techniques would increase the coverage of the cloud-top measurements to many more partially cloudy pixels. Another improvement would be to choose the atmospheric correction value listed in Table I by using coincident sounding channels (e.g. from TOVS) or model profiles to determine the total column water amount. This would help to ensure that the atmospheric correction term was more representative of the actual conditions present during the satellite overpass. Eyre *et al.* (1984) also suggest that the magnitude of the brightness temperature difference between AVHRR channels 3 and 4 may be an indicator of fog thickness which is another parameter which could be included along with the cloud-top temperature.

In the future (mid 1990s) the second-generation Meteosat series will become operational. They will have many of the advantages of the current AVHRR instrument and the capability of making at least half-hourly measurements over the British Isles allowing the time evolution of the cloud or fog top to be monitored. A scheme similar to the one described above could be employed to derive cloud-top parameters from second-generation Meteosat data.

Acknowledgements

I thank G. Dehal (University of Oxford) for carrying out the atmospheric transmittance calculations and J.N. Ricketts (Meteorological Office) for useful discussions and providing the data for the fog case-study. The raw HRPT data was supplied by the Lasham and University of Dundee receiving stations.

References

Bowen, R.A.	1982	The meteorological product: 'Cloud-Top Height'. *Eur Space Agency Bull*, **30**, 16–20.
Browning, K.A., Bader, M.J. Waters, A.J., Young, M.V. and Monk, G.A.	1987	Application of satellite imagery in nowcasting and very short range forecasting. *Meteorol Mag*, **116**, 161–179.
Edwards, D.P.	1987	The new Oxford line by line atmospheric transmission model, GENLN2. *In* Report of Atmospheric Spectroscopy Applications Workshop, RAL, 1–3 Sept, 1987.
Eyre, J.R., Brownscombe, J.L. and Allam, R.J.	1984	Detection of fog at night using Advanced Very High Resolution Radiometer (AVHRR) imagery. *Meteorol Mag*, **113**, 266–271.
Eyre, J.R. and Menzel, W.P.	(1988)	Retrieval of cloud parameters from satellite sounder data. (Submitted to *J Clim Appl Meteorol.*)
Findlater, J., Roach, W.T. and McHugh, B.C.	(1988)	The Haar of northeast Scotland. (Submitted to *Q J R Meteorol Soc.*)
Inoue, T.	1985	On the temperature and effective emissivity determination of semi-transparent cirrus clouds by bi-spectral measurements in the 10 μm window region. *J Meteorol Soc Japan*, **63**, 88–98.
Kriebel, K.T., Moerl, P., Reinhardt, M.E., Schellhase, R., Koenig, T. and Rattei, W.	1983	Comparison of cloud top heights measured by airborne lidar and TIROS-N image data. *Adv Space Res*, **2**, No. 6, 11–13.
Pescod, R.W., Saunders, R.W. and Eyre, J.R.	1986	Sea surface temperature images from Advanced Very High Resolution Radiometer (AVHRR) data. *Meteorol Mag*, **115**, 318–325.
Saunders, R.W. and Pescod, R.W.	1988	A users guide to the APOLLO scheme on HERMES/HOMER. (Unpublished, copy available in the National Meteorological Library, Bracknell.)
Saunders, R.W. and Kriebel, K.T.	1988	An improved method for detecting clear sky and cloudy radiances from AVHRR data. *Int J Remote Sensing*, **9**, 123–150.
Szejwach, G.	1982	Determination of semi-transparent cirrus cloud temperature from infrared radiances. Application to METEOSAT. *J Appl Meteorol*, **21**, 384–393.
Turner, J., Allam, R.J. and Maine, D.R.	1986	A case study of the detection of fog at night using channels 3 and 4 on the Advanced Very High Resolution Radiometer (AVHRR). *Meteorol Mag*, **115**, 285–290.

551.506.1(41-4)

The autumn of 1987 in the United Kingdom

G.P. Northcott

Meteorological Office, Bracknell

Summary

The autumn was generally cool and wet in the south, although somewhat drier in Scotland. The main features of note were the violent storm on 16 October followed by the flooding in Wales and Northern Ireland on the 17th and 20th respectively.

1. The autumn as a whole

Rainfall amounts were above normal in all districts of England and Wales, partly as a result of East Anglia, southern and eastern England and South Wales all having had more than twice the normal rainfall for October, whereas in Scotland rainfall amounts were slightly below normal and in Northern Ireland about normal. Sunshine amounts were near average over Scotland as a whole, average over England and Wales and above average over Northern Ireland. Mean temperatures were about normal in England and Wales, but about 0.5 °C below normal in Scotland and Northern Ireland.

Information about the temperature, rainfall and sunshine during September–November 1987 is given in Fig. 1 and Table I.

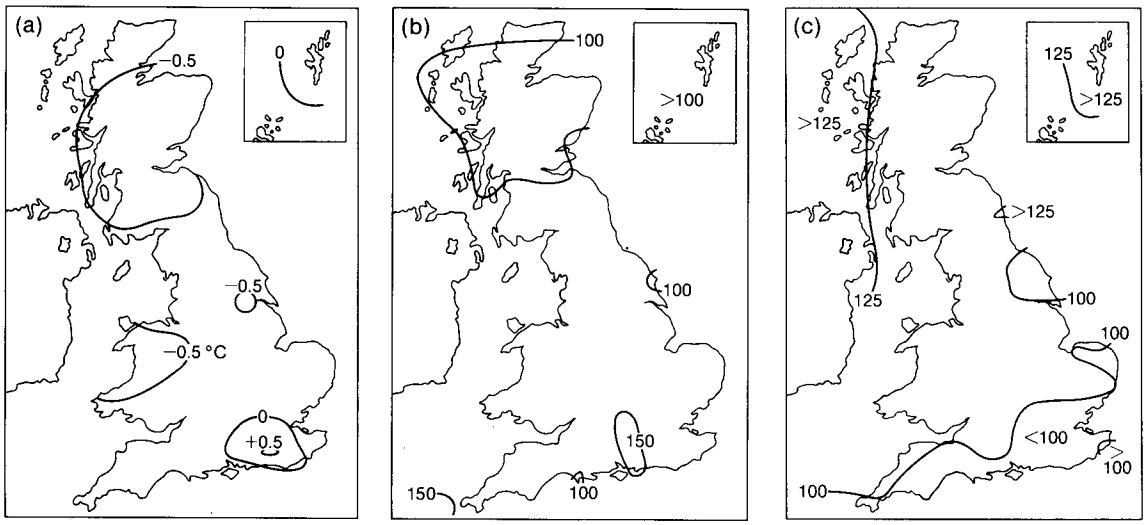

Figure 1. Values of (a) mean temperature difference, (b) rainfall percentage and (c) sunshine percentage for autumn 1987 (September–November), relative to 1951–80 averages.

October. October was a very cool month with mean temperatures below normal everywhere apart from one or two places in southern England, and ranged from about 2 °C below normal in parts of central Scotland to near normal in parts of southern England. It was an exceptionally wet month; provisional figures suggest that it was the third wettest October in England and Wales since records began in 1727. Rainfall amounts ranged from about normal in north-west Scotland to three times the normal in parts of the south and east of England. Sunshine amounts were above normal in most areas, the notable exceptions being parts of the south coast of England, and northern England and eastern areas of Scotland where it was rather dull overall; amounts ranged from 80% in the Isle of Wight to more than 150% in the Western Isles of Scotland.

November. Mean monthly temperatures were near normal everywhere in the United Kingdom and ranged from 0.5 °C above normal in Shetland to 0.4 °C below normal at Aberporth, Dyfed. Monthly rainfall values for all districts were below normal, although one or two places had considerably more than the monthly average; amounts ranged from more than 130% at Brize Norton, Oxfordshire to just over 40% at Edinburgh. Sunshine amounts were below normal in most areas except parts of southern and eastern Scotland, south-west England and west Wales where it was quite sunny; totals ranged from about 60% in central England to 148% at Aberporth, Dyfed.

2. The individual months

September. Monthly mean temperatures were below normal in the north and above normal in the south, ranging from 0.9 °C above normal in parts of southern England to 0.7 °C below normal in southern Scotland. Rainfall totals were mainly below normal in England and Wales, but above normal in parts of western Scotland, ranging from a very dry 26% in the Isle of Wight to 153% in the Outer Hebrides. Sunshine totals for the month were generally above average apart from central southern and south-west England where they were about normal or below; amounts ranged from 158% in Shetland to 68% in the Isles of Scilly.

Table I. *District values for the autumn months, September–November 1987, relative to 1951–80 averages*

District	Mean temperature (°C)	Rain-days	Rainfall	Sunshine
	Difference from average		Percentage of average	
Northern Scotland	−0.3	+1	98	108
Eastern Scotland	−0.6	−1	96	107
Eastern and north-east England	−0.2	−2	118	104
East Anglia	+0.1	+2	137	95
Midland counties	−0.2	+2	125	97
South-east and central southern England	−0.2	+2	135	94
Western Scotland	−0.6	+2	107	116
North-west England and North Wales	−0.3	+1	114	105
South-west England and South Wales	−0.2	+2	125	102
Northern Ireland	−0.6	0	100	126
Scotland	−0.5	+1	94	110
England and Wales	−0.1	+1	123	100

Highest maximum: 26.5 °C in south-east and central southern England in September.
Lowest minimum: −7.6 °C in western Scotland in November.

3. The weather month by month

September. The month began with thundery rain moving slowly eastwards on the 1st, bringing heavy rain to counties to the north and west of London during the night with reports of flooding. It remained unsettled with showers or longer periods of rain at times, becoming widespread on the 11th and 12th as the remnant of tropical storm Cindy crossed central areas of the United Kingdom. Northern parts of the United Kingdom were showery for the next six days, while it became dry in central and southern areas, but later on the 16th and early on the 17th wet weather came to parts of England and Wales. After a dry day in all areas on the 18th it was mostly dry on the 20th, but on the next two days it was wet in the west. Apart from a few showers, mainly in northern England, the rest of the month was dry, though cool. Thunderstorms developed over eastern England and south-eastern Scotland on the 5th, and over south-east England on the 19th. It was showery in most areas on the 23rd and 24th with some hail and thunder, especially in central and south-eastern England. Hail was widespread over the United Kingdom during the 24th and 25th. It was the sunniest September at Tiree, Strathclyde since records began there in 1927 and the second sunniest at Lerwick, Shetland in a record back to 1922, while it ranked third in Edinburgh and Auchincruive, Strathclyde in records back to 1901 and 1932 respectively. In Northern Ireland only September 1986 was sunnier since 1941.

October. After a dry start to October it became changeable with a great deal of rainfall in the first half of the month, bringing widespread flooding to the south and east. Winds became strong to gale force on the 7th and 8th and remained strong until the 11th. On the 9th torrential rain caused flooding and road accidents in south-eastern areas as gales swept the south coast; floods brought commuter traffic leaving London to a standstill, with road tunnels and underpasses, including the London/Heathrow Airport access road, closed. Heavy rain caused severe flooding in many parts of the south-east on the 10th; in Essex some villages were almost cut off when the River Stour burst its banks after more than 50 mm of rain fell in less than 24 hours. Flooding to a depth of 4 metres was reported near Colchester. The storm on the 16th brought violent-storm-force winds and heavy rain to southern England causing chaos. Millions of trees were uprooted or had branches broken off and many crashed

into power lines, leaving a large number of homes without electricity, some for as long as a fortnight, and causing severe disruption to traffic. During the passage of the storm, several gusts of more than 90 kn were recorded across the south-eastern corner of England — 100 kn was recorded at Shoreham-by-Sea, West Sussex. On the night of the 17th/18th there were strong winds and widespread flooding in western and northern areas of Wales; substantial amounts of rain fell in western parts of Wales. Trecastle, Powys recorded 222 mm of rain over the five days from the 14th to 18th, 77 mm more than the monthly normal. Flooding was worst around Carmarthen and the areas of the Rivers Teifi and Tywi; one of the supports of the railway bridge over the River Tywi at Glanrhyd, near Llandeilo was damaged by flood water and debris and a Swansea to Shrewsbury train plunged into the river with the loss of four lives. On the 20th torrential rain brought flooding to large areas of Northern Ireland with flood water nearly 3 m deep in the town of Strabane, Co. Londonderry and extensive flooding in Co. Tyrone and Co. Fermanagh. It remained unsettled for the last week or so, though with some fine and sunny interludes, but gradually become cooler. Hampstead, Greater London reported the wettest October since records began there in 1903. Thunder was heard over a very wide area on the 5th and in western areas around the 17th.

November. November began generally dry except in Orkney and Shetland, but during the first week unsettled weather returned to all parts. The south-eastward passage of the depression across western areas of the United Kingdom on the 8th brought heavy rain to some places. After a brief drier interval, there was a change to an unsettled westerly airstream on the 10th, with rain or showers in most areas although with some drier spells, until the 25th, when brighter weather came to the north-west, spreading to the south-east by the 27th. Further rain reached all areas except south-eastern England on the 29th, with substantial falls in Devon, Cornwall and Dyfed. The 30th was a dry day except in the Midlands and north-east England. Thunderstorms were reported here and there on several days, with an outbreak over the Bristol Channel on the 12th. Hail was widespread between the 10th and 13th, and 22nd and 25th.

551.515.81:551.577.2

Modelling precipitation in a cold frontal rainband*

G.P. Cox†

Meteorological Office, Bracknell

Summary

A study is made of the ability of a simple 'warm' parametrization scheme (solid phase not taken into account) to represent adequately the microphysical processes acting in a cold frontal rainband. The numerical simulations indicate that a mixed-phase parametrization is required in dynamical models of high resolution.

1. Introduction

Studies of frontal rainbands have highlighted the need for a better understanding of the influence of precipitation processes upon their dynamical structure. Since feedback may occur through diabatic processes (e.g. evaporation and melting) as well as precipitation loading (i.e. the effect of precipitation drag on the surrounding air), it seems likely that the effects become substantial locally. The

* An abridged version of a paper by Cox (1988) which appeared in the *Quarterly Journal of the Royal Meteorological Society*.

† Now at Software Sciences Ltd, Farnborough, United Kingdom.

microphysical processes acting in the production of rainfall are not fully understood and there is considerable doubt over the degree to which these complex processes can, or should, be represented or parametrized in computer models which resolve the mesoscale. The main aspect of this study concerns the ability of a highly parametrized 'warm' microphysical scheme (i.e. one with explicit representation of rain and cloud water but no representation of the solid phase) to simulate precipitation-induced feedbacks in dynamical models of high resolution (< 15 km). Such a scheme is attractive because it requires much less computer space and time than an ice or mixed-phase parametrization and is likely to be easily tuned.

In this study a comparison is made between the results of a two-dimensional diagnostic model using:

(a) a full parametrization scheme based on that presented by Rutledge and Hobbs (1983, 1984), and

(b) the 'warm' microphysical parametrization of Tripoli and Cotton (1980).

The microphysical processes represented by these schemes are shown schematically in Fig. 1.

Here a brief description is given of how the two schemes compare when they are applied to a narrow cold frontal rainband. Further details of the results can be found in Cox (1988); this also contains a report of the corresponding results for a frontal rainband which has vertical motions that are weak and uniform over horizontal distances of 100 km or more.

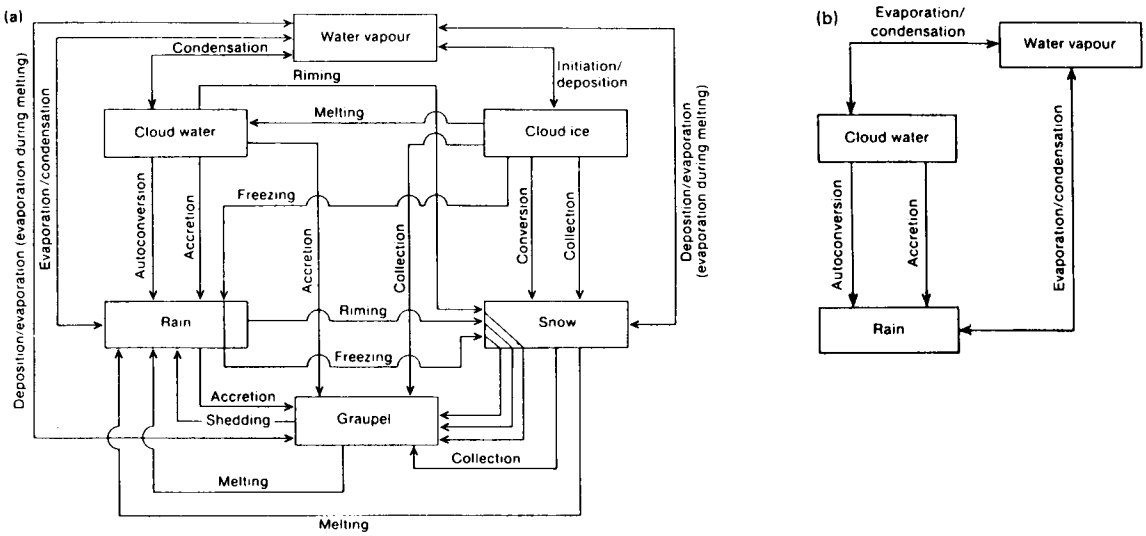

Figure 1. Schematic diagram depicting (a) the cloud and precipitation processes included in the full microphysical parametrization and (b) the processes included in the warm microphysical scheme.

2. The model

The model used in this study is similar to that described by Rutledge and Hobbs (1983, 1984). It is a two-dimensional diagnostic model in the x–z plane, where x is the horizontal distance perpendicular to the front and z is the height coordinate. The model variables fall into two categories:

(a) The horizontal wind, vertical velocity and pressure are specified and held constant during the numerical simulation.

(b) The temperature and mixing ratios of water vapour, cloud water, cloud ice, snow, rain and graupel are allowed to vary throughout the simulation, according to the thermodynamic equation and the conservation equations of the various mixing ratios, until a steady state is reached.

The conservation equations used in the model all have the same form. If χ is a mixing ratio, the conservation equation has the form

$$\frac{\partial \chi}{\partial t} = -u\frac{\partial \chi}{\partial x} - w\frac{\partial \chi}{\partial z} - \frac{1}{\rho}\frac{\partial}{\partial z}(\rho V \chi) + \frac{S}{\rho}$$

where u and w are the horizontal and vertical velocities of the air, ρ is the air density, V is the fallspeed of the precipitation (applies to rain, snow and graupel) and S represents the sources and sinks. The sources and sinks and the fallspeed have to be parametrized — the details are given in the papers already cited in section 1.

The non-zero fallspeed of the precipitation means that rain, snow and graupel move with the horizontal wind whilst falling relative to the updraught. However, cloud water and cloud ice have zero fallspeed and so they are simply advected by the airflow.

3. Model results

3.1 *Full microphysics*

The initial prescribed stream function over the 24 km × 3.5 km domain is shown in Fig. 2. The wind fields are based upon observations of narrow cold frontal rainbands by Browning and Harrold (1970) and Hobbs and Persson (1982).

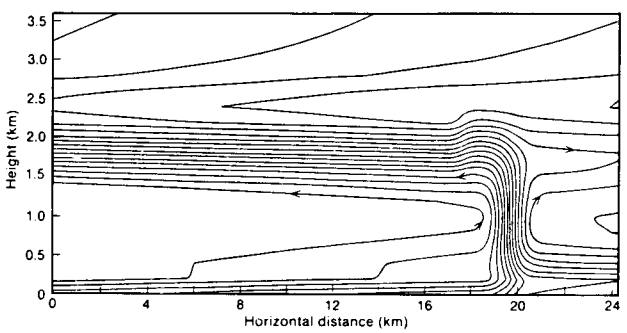

Figure 2. Prescribed stream function in the cold frontal simulation.

The results using the full microphysical parametrization scheme are shown in Fig. 3. The pattern of surface precipitation is almost the same as that observed by Hobbs and Persson (1982) with peak rates of 12 mm h^{-1} occurring about 4 km behind the surface cold front (Fig. 3(a)). Precipitation in the updraught is mainly carried up over the cold air but a fraction is transported back into the warm sector. Such a reverse flow is not uncommon and has been observed by Browning and Harrold (1970) and Hobbs and Persson (1982). This flow increases precipitation efficiency locally by allowing snow to cycle through the updraught. The snow can then grow by accretion and deposition removing cloud water and vapour which might otherwise be advected away from the front at high levels.

The heating rates associated with the diabatic effects are shown in Fig. 3(b). The configuration of the flow, with the updraught outflow overriding the cold air and allowing the precipitation to fall into it and evaporate, is ideally suited to maintaining heat sinks behind the front.

The distribution of the cloud water mixing ratio is given in Fig. 3(c). In many studies of cold frontal zones the region of cold air behind the front is compared to a classical density current. From a consideration of the propagation equation of a density current (Cox 1988) it can be shown that the current's velocity may be increased by around 10% by the action of differential precipitation loading

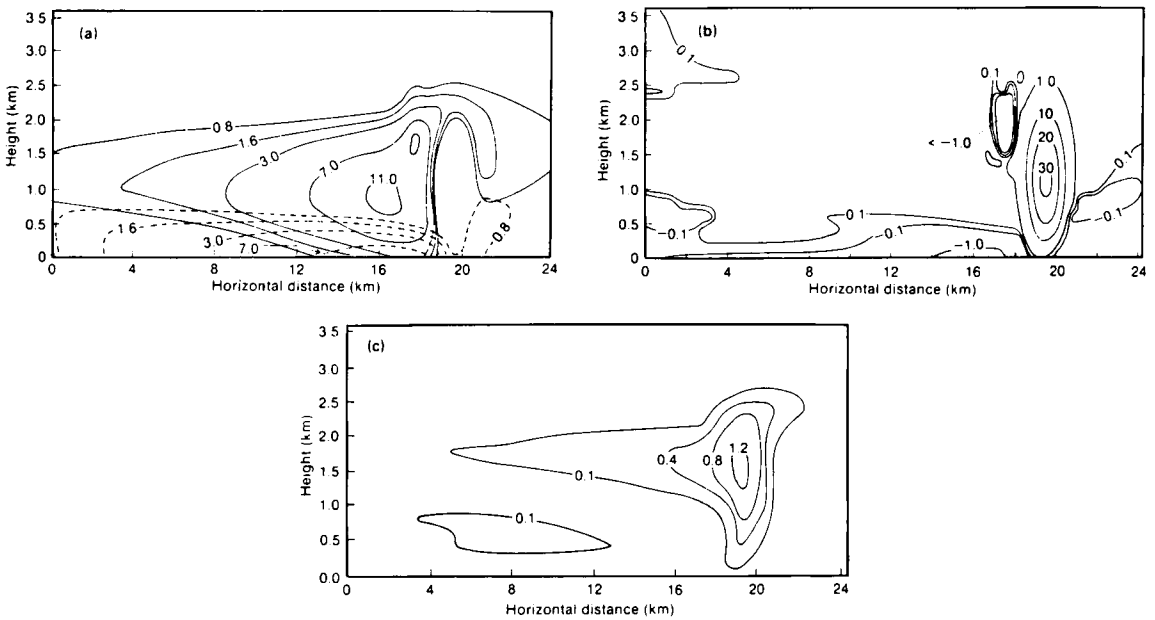

Figure 3. Results from the full microphysical parametrization for (a) precipitation rate (mm h^{-1}), solid lines represent snow (melted equivalent) and dashed lines represent rain, (b) latent heating rate (10^{-3} K m^{-3} s^{-1}) and (c) cloud water mixing ratio (g kg^{-1}).

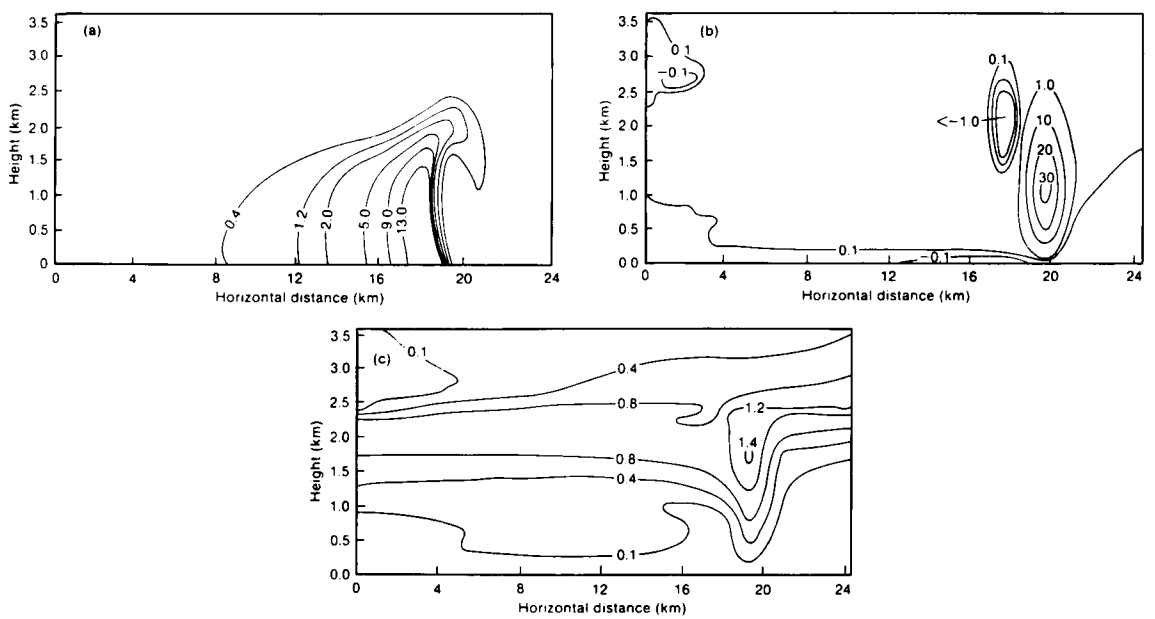

Figure 4. As Fig. 3 but for the warm microphysical parametrization.

seen in these results. The weight of precipitation behind the frontal zone may be an important factor in determining frontal speed.

3.2 *Warm microphysics*

Fig. 4 shows results from the simulation using the warm microphysical scheme. Since rain falls faster than either snow or graupel there is a very concentrated precipitation maximum close to and behind the surface cold front with the maximum rate exceeding 18 mm h^{-1} (Fig. 4(a)). The cloud liquid water content in the narrow updaught is in accord with observations, but the general value at 2 km (0.8 g kg^{-1}) is higher than observed (Fig. 4(c)). This can be reduced by increasing the parametrized accretion and autoconversion rates but the amount of precipitation inevitably increases. The difference in fallspeed of the various hydrometeor species leads to quite different patterns of mass loading between the two simulations. The major problem with the warm microphysics is the erroneous cloud water at 2 km. Here there is no division between small ice and snow in the full ice microphysics case corresponding to the division between cloud drops and rain in the warm case. Hence the accumulation of cloud particles is less likely to occur with ice microphysics. Since latent heat release is dominated by the condensation of water vapour to cloud water in both simulations, heating rates are generally rather similar (compare Figs 4(c) and 3(c)) except in and below the melting layer.

4. Conclusions

The simulation of the narrow cold frontal rainband using the full (mixed-phase) parametrization gave results comparable with field observations. However, the warm microphysics parametrizations gave less realistic distributions of surface precipitation and precipitation concentration aloft. Since melting and loading effects may provide important feedbacks to the dynamics locally, a highly parametrized warm scheme is likely to be inadequate for dynamical models of high resolution. In corresponding results for a weak warm frontal rainband (Cox 1988) similar conclusions were drawn. In addition, the warm microphysical parametrization did not represent the distribution of latent heat transfer well, particularly at levels where particle melting occurred using the ice phase parametrization.

References

Browning, K.A. and Harrold, T.W. 1970 Air motion and precipitation at a cold front. *Q J R Meteorol Soc*, **96**, 369–389.

Cox, G.P. 1988 Modelling precipitation in frontal rainbands. *Q J R Meteorol Soc*, **114**, 115–127.

Hobbs, P.V. and Persson, P.O.G. 1982 The mesoscale and microscale structure and organization of clouds and precipitation in midlatitude cyclones. Part V: The substructure of narrow cold-frontal rainbands. *J Atmos Sci*, **39**, 280–295.

Rutledge, S.A. and Hobbs, P.V. 1983 The mesoscale and microscale structure and organization of clouds and precipitation in midlatitude cyclones. Part VIII: A model for the 'seeder-feeder' process in warm-frontal rainbands. *J Atmos Sci*, **40**, 1185–1206.

1984 The mesoscale and microscale structure and organization of clouds and precipitation in midlatitude cyclones. Part XII: A diagnostic modeling study of precipitation development in narrow cold-frontal rainbands. *J Atmos Sci*, **41**, 2949–2972.

Tripoli, G.J. and Cotton, W.R. 1980 A numerical investigation of several factors contributing to the observed variable intensity of deep convection over South Florida. *J Appl Meteorol*, **19**, 1037–1063.

551.5:92

W.H. Hogg (1910–87) — an appreciation

J.A. Taylor

University College of Wales, Aberystwyth

'Bill' Hogg was born in Fulham and attended Westminster City School. He graduated in geology (1932) and geography (1934) at University College London. Whilst at university he met the late Marjorie Hutchinson whom he married in 1936.

Following various teaching and research commitments, he joined the Meteorological Office in 1939 as a Temporary Technical Assistant and served in various locations, amongst them Bristol, Upavon, Germany and Headquarters. For the major part of his service he specialized in climatology and agroclimatology, with a spell between 1949 and 1953 as a forecaster in the 2nd Tactical Air Force in Germany. He was promoted to the grade of Principal Scientific Officer in 1957.

Shortly after the end of the Second World War, the then Director of the Meteorological Office (Sir Nelson Johnson) initiated moves aimed at rendering the service of the Office more relevant to a wide variety of user-interests. Amongst these was the Ministry of Agriculture, Fisheries and Food which was engaged, at that time, in consolidating and expanding the advisory functions, some research, and statutory duties which had been performed during hostilities from a network of Regional, County and District Offices of the War Executive Committees, so creating a new organization entitled the National Agricultural Advisory Service (NAAS). Certain members of the Office were posted to a selection of these regional centres, amongst them Bill Hogg who headed the Bristol centre from 1953 to his retirement in 1971. He was eminently suited to such a post, both personally and technically, and earned an enviable and widely appreciated reputation for forging links between the increasing specialism of meteorology and the appliction of results in the field.

I was fortunate that my early involvement in agroclimatological research led me to seek the advice of three members of the Meteorological Office who were successfully pioneering and establishing agrometeorological services for British farmers. These were Lionel Smith, Ron Gloyne and Bill Hogg, all of whom had a combination of natural skills in applied science with a capacity for communicating on practical issues with farmers and growers. At my invitation all three, Bill Hogg in particular, became regular contributors to the Annual Series of Symposia in Agricultural Climatology which I convened at the University College of Wales, Aberystwyth between 1958 and 1973. We learned so much from spontaneous interdisciplinary exchanges and the ensuing memoranda and books which the Series generated. We reached a wide audience both nationally and internationally. In 1972 Bill and I established 'Environmental Consultants' which continues to prosper, due not least to Bill's major contributions on such consultancies as the fog potential of proposed alternative motorway routes, the best sites for developments in viticulture in south central England and agroclimatological advice for specific farmers and specific enterprises.

During his career he published a number of scientific papers, some solely in his name, some in collaboration with others. In 1965 he was awarded the Royal Meteorological Society Darton Prize.

Amongst his many activities during his retirement were a course of lectures at the University of Bristol and, in particular, the chairmanship of the Bristol and District Branch of the Civil Service Retirement Fellowship, which he held from March 1978 to March 1986.

Bill Hogg's professional and personal contributions to the cause of applied agroclimatology were of a very high order. He combined a meticulous discipline with a warmth of communication with colleague

and customer alike. He combined a penetrating pragmatism with a sympathetic, yet scientific, ability to solve real-world agroclimatological problems. I count it a rare privilege to have known and worked with him, as a friend and colleague. He will be sadly missed by all those who knew him.

He is survived by a daughter, Ruth, and five grandchildren.

Awards

L.G. Groves Memorial Prizes and Awards for 1986

The L.G. Groves Memorial Prizes and Awards were endowed by Major and Mrs Keith Groves in memory of their son Sergeant Louis Grimble Groves, RAFVR, who lost his life in September 1945 while serving as an Air Meteorological Observer with 517 Squadron Coastal Command. The 1986 awards were presented by Mr Andrew Douglas-Bate, a relative through marriage of the Groves family, at HQ Strike Command (High Wycombe) on 26 November 1987. Air Vice-Marshal R.A.F. Wilson, AFC, SASO HQ Strike Command, presided and the citations were read by Squadron Leader J.W. White of the Flight Safety Inspectorate. The ceremony was also attended by members of the Groves family, representatives of the RAF and the Meteorological Office, and the wives of the recipients of the awards. This year's ceremony marked the 40th anniversary of the first presentations which took place on 8 October 1947.

Dr S. Nicholls, winner of the Meteorology Prize, receives a mantle clock from Mr A. Douglas-Bate.

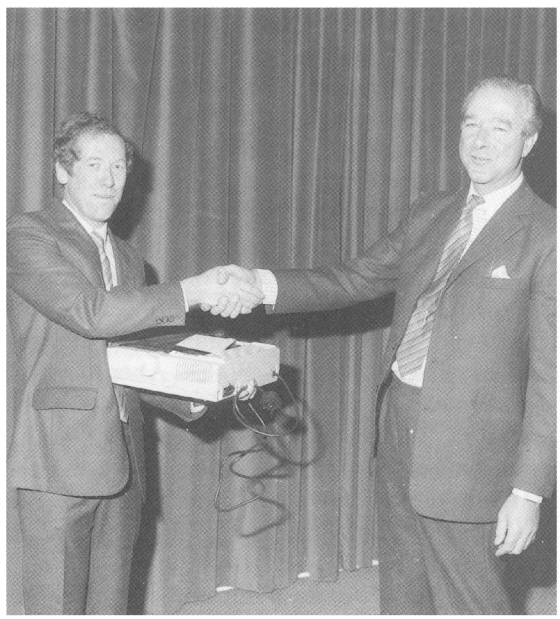

Mr G. Cooper, winner of the Award for Meteorological Observation, receives a printer for a home computer from Mr A. Douglas-Bate.

Meteorology Prize — Dr S. Nicholls

The citation read as follows:

> To Dr S. Nicholls for his perceptive use of measurements from the Meteorological Research Flight Hercules aircraft to reveal the relationship between the radiative, turbulent and microphysical properties of the stratocumulus layer clouds and their effects on the evolution of the clouds. An understanding of these relationships is essential for forecasting the presence of clouds and their effects on surface temperature and fog formation, as well as the correct representation of layer cloud in numerical forecasting and climate models.

Dr Steve Nicholls has been involved in several international experiments using the Hercules, including the GARP Atlantic Tropical Experiment, the Joint Air-Sea Interaction Project and, more recently, the First ISCCP Regional Experiment. In addition to his work on the interpretation of aircraft data, he has been involved in the development of numerical models of clouds and with the development of a fast-response instrument to measure the total water content in cloudy and cloud-free air. He joined the Office in 1973 and was posted to the Meteorological Research Flight (MRF) at Farnborough from 1974 to 1982. During this period he also spent a year in the United States working at the National Center for Atmospheric Research in Colorado. On promotion to Principal Scientific Officer in 1982 he joined the Cloud Physics Branch where he combined his expertise on turbulence measurements with the Branch's expertise on cloud microphysics.

Award for Meteorological Observation — G. Cooper

The citation for this award was as follows:

> To Mr G. Cooper for his important contribution in installing, testing, modifying and operating many of the instruments which make the Hercules aircraft of the Meteorological Research Flight one of the best equipped meteorological research aircraft available. His work on the droplet sampling instrument in particular called for a wide range of expertise and led to major improvements in accuracy and reliability of the measurements.

Graham Cooper joined the Meteorological Office in 1968. He worked at MRF from 1969 to 1971 and was involved in measurements of sea surface temperature and the design of an instrument to measure water droplet sizes and distributions in clouds. There then followed a period working in various Branches and outstations, but in 1977 he returned to MRF where he again got involved in developing airborne droplet-sizing instruments. In 1980 he joined the Cloud Physics Branch, and worked on the improvement of the droplet-sizing instrumentation and the development of an analysis system for the holograms taken during airborne experiments. Also, whilst working with Steve Nicholls, he contributed to the design and feasibility testing of a rapid-response total-water content meter which is now in the process of being fitted to the Hercules.

Air Safety Prize and Ground Safety Award

Flight Lieutenant N.B. Goulding from RAF Linton-on-Ouse received the Air Safety Prize in recognition of his work on an improved method of escape through the canopy of a Bulldog aircraft. The judges felt that the submissions for the Ground Safety Award did not quite reach the standards usually expected and so no award was made.

Satellite and radar photograph — 0600 GMT 26 May 1988

The picture covering much of western Europe shows radar data from several countries superimposed on infra-red cloud imagery from Meteosat.

Two bands of frontal cloud and rain are present lying north to south from central Britain to central France. The western band is related to a slow-moving surface front, whilst the eastern band formed during the previous 24 hours within a zone of increasing baroclinicity as warm air over the Mediterranean advected northwards in a southerly flow aloft. The eastern front was therefore drawn by the UK Central Forecasting Office as an upper front. Much of the cloud and precipitation within this band is of convective origin. The front to the west is generally feeble in terms of precipitation. However, the pulse of moderate to heavy rain over Wales (moving north) is associated with a shallow surface wave. The wave had been induced just ahead of a region of enhanced convection, the axis of which is marked as a surface cold front.

Isolated thunderstorms occurring over The Netherlands and eastern France are shown by the localized areas of heavy rain. Outside the area of radar coverage, the region of cold topped cloud (dark blue) almost certainly represents a thunderstorm.

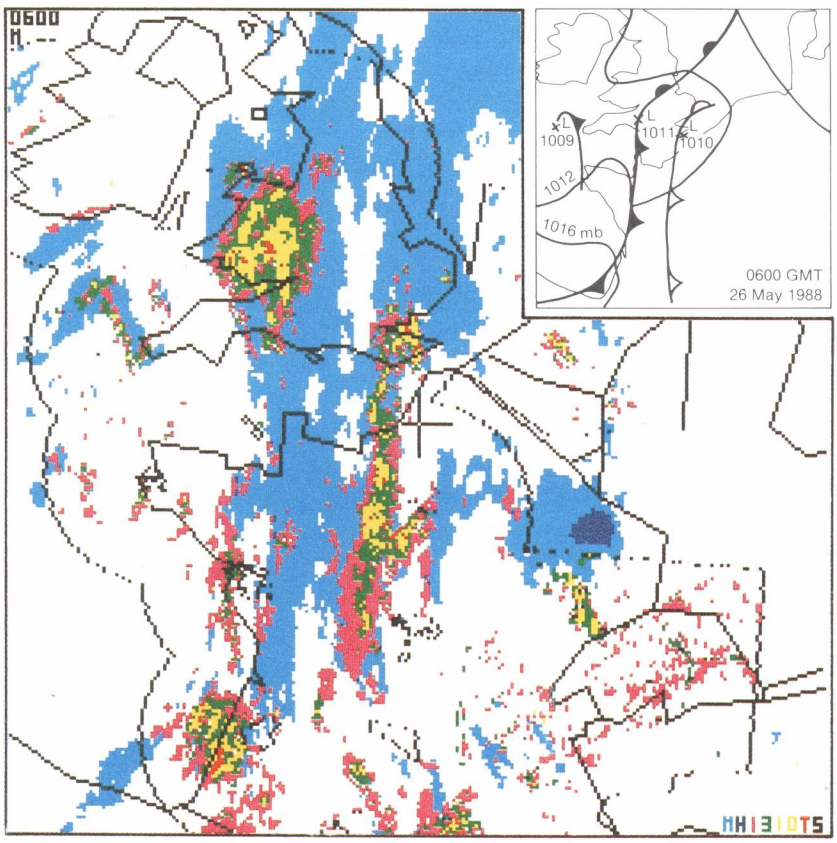

Key. Infra-red cloud-top temperatures (°C): light blue < -15, dark blue < -35. Radar rainfall (mm h^{-1}): pink < 1, green 1–3, yellow 3–10, and red > 10. Coastlines: National boundaries and radar network boundaries are shown in black. The small regions enclosed in black over France are regions of permanent echo. (Much of the apparently light precipitation over Switzerland is also permanent echo or anomalous propagation).

Meteorological Magazine

GUIDE TO AUTHORS

Content

Articles on all aspects of meteorology are welcomed, particularly those which describe the results of research in applied meteorology or the development of practical forecasting techniques.

Preparation and submission of articles

Articles for publication and all other communications for the Editor should be addressed to the Director-General, Meteorological Office, London Road, Bracknell, Berkshire RG12 2SZ and marked 'For *Meteorological Magazine*'.

Articles, which must be in English, should be typed, double-spaced with wide margins, on one side only of A4-size paper. Tables, references and figure captions should be typed separately.

Spelling should conform to the preferred spelling in the *Concise Oxford Dictionary*.

References should be made using the Harvard system (author, date) and full details should be given at the end of the text. If a document referred to is unpublished, details must be given of the library where it may be seen. Documents which are not available to enquirers must not be referred to.

Tables should be numbered using roman numerals and provided with headings. We consider vertical and horizontal rules to be unnecessary in a well-designed table; spaces should be used instead.

Mathematical notation should be written with extreme care. Particular care should be taken to differentiate between Greek letters and Roman letters for which they could be mistaken. Double subscripts and superscripts should be avoided, as they are difficult to typeset and difficult to read. Keep notation as simple as possible; this makes typesetting quicker and therefore cheaper, and reduces the possibility of error. Further guidance is given in BS1991: Part 1: 1976 and *Quantities, Units and Symbols* published by the Royal Society.

Illustrations

Diagrams must be supplied either drawn to professional standards or drawn clearly, preferably in ink. They should be about 1½ to 3 times the final printed size and should not contain any unnecessary or irrelevant details. Any symbols and lettering must be large enough to remain legible after reduction. Explanatory text should not appear on the diagram itself but in the caption. Captions should be typed on a separate sheet of paper and should, as far as possible, explain the meanings of the diagrams without the reader having to refer to the text.

Sharp monochrome photographs on glossy paper are preferred: colour prints are acceptable but the use of colour within the magazine is at the Editor's discretion. In either case contrast should be sufficient to ensure satisfactory reproduction.

Units

SI units, or units approved by WMO, should be used.

Copyright

Authors wishing to retain copyright for themselves or for their sponsors should inform the Editor when they submit contributions which will otherwise become UK Crown copyright by right of first publication.

It is the responsibility of authors to obtain clearance for any copyright material they wish to use before submitting it for publication.

Free copies

Three free copies of the magazine are provided for authors of articles published in it. Separate offprints for each article are not provided.

Meteorological Magazine

July 1988

Vol. 117
No. 1392

CONTENTS

Contributions: It is requested that all communications to the Editor and books for review be addressed to the Director-General, Meteorological Office, London Road, Bracknell, Berkshire RG12 2SZ, and marked 'For *Meteorological Magazine*'. Contributors are asked to comply with the guidelines given in the *Guide to authors* which appears on the inside back cover. The responsibility for facts and opinions expressed in the signed articles and letters published in *Meteorological Magazine* rests with their respective authors. Authors wishing to retain copyright for themselves or for their sponsors should inform the Editor when submitting contributions which will otherwise become UK Crown copyright by right of first publication.

Subscriptions: Annual subscription £27.00 including postage; individual copies £2.30 including postage. Applications for postal subscriptions should be made to HMSO, PO Box 276, London SW8 5DT; subscription enquiries 01–211 8667.

Back numbers: Full-size reprints of Vols 1–75 (1866–1940) are available from Johnson Reprint Co. Ltd, 24–28 Oval Road, London NW1 7DX. Complete volumes of *Meteorological Magazine* commencing with volume 54 are available on microfilm from University Microfilms International, 18 Bedford Row, London WC1R 4EJ. Information on microfiche issues is available from Kraus Microfiche, Rte 100, Milwood, NY 10546, USA.

ISBN 0 11 728086 0

ISSN 0026–1149

Printed in the United Kingdom for Her Majesty's Stationery Office
Dd 0240021 C13 6/88 3936 12521